

# Surface homogenization of an array of Helmholtz resonators for a viscoacoustic model using two-scale convergence

Kersten Schmidt<sup>a</sup>, Adrien Semin<sup>a</sup>

<sup>a</sup>: Technische Universität Darmstadt, Fachbereich Mathematik, AG Numerik und  
Wissenschaftliches Rechnen, Dolivostrasse 15, 64293 Darmstadt, Germany

**Corresponding author:** Kersten Schmidt, Technische Universität Darmstadt, Fachbereich Mathematik, AG Numerik und Wissenschaftliches Rechnen, Dolivostrasse 15, 64293 Darmstadt, Germany  
E-mail: kschmidt@mathematik.tu-darmstadt.de

## Abstract

We derive the weak limit of a linear viscoacoustic model in an acoustic liner that is a chamber connected to a periodic repetition of elongated chambers – the Helmholtz resonators. As model we consider the time-harmonic and linearized compressible Navier-Stokes equations for the acoustic velocity and pressure. Following the approach in Schmidt *et al.*, J. Math. Ind 8:15, 2018 for the viscoacoustic transmission problem of multiperforated plates the viscosity is scaled as  $\delta^4$  with the period  $\delta$  of the array of chambers and the size of the necks as well as the wall thickness like  $\delta^2$  such that the viscous boundary layers are of the order of the size of the necks. Applying the method of two-scale convergence we obtain with a stability assumption in the limit  $\delta \rightarrow 0$  that the acoustic pressure fulfills the Helmholtz equation with impedance boundary conditions. These boundary conditions depend on the frequency, the length of the resonators and through the effective Rayleigh conductivity – that can be computed numerically – on the shape of their necks. We compare the limit model to semi-analytical models in the literature.

## Keywords

asymptotic analysis; periodic surface homogenization; singular asymptotic expansions; stress intensity factor.

**AMS Subject Classification** 32S05, 35C20, 35J05, 35J20, 41A60, 65D15

## Contents

<b>1</b>	<b>Introduction</b>	<b>2</b>
<b>2</b>	<b>Description of the problem and main results</b>	<b>4</b>
2.1	Description of the problem . . . . .	4
2.2	Effective Rayleigh conductivity . . . . .	5
2.3	Weak convergence to a limit problem with impedance boundary conditions . . . . .	7
<b>3</b>	<b>Proof of the weak convergence to the limit</b>	<b>9</b>
3.1	Weak convergence in the resonator array . . . . .	10
3.2	Weak convergence in the pattern below aperture . . . . .	14

3.3	Weak convergence in the apertures . . . . .	16
3.4	Weak convergence in the pattern above aperture . . . . .	19
3.5	Weak convergence in the macroscopic region . . . . .	21
3.6	Uniqueness of the limit . . . . .	22
<b>4</b>	<b>Numerical simulations</b>	<b>23</b>
4.1	Numerical computation of the effective Rayleigh conductivity . . . . .	23
4.2	Study of the acoustic impedance and local resonance frequency . . . . .	24
4.3	Dissipation by an array of Helmholtz resonators in a duct . . . . .	26
<b>5</b>	<b>References</b>	<b>29</b>

## 1 Introduction

The noise emission from aircraft gas turbines, car engines and several other industrial applications is a matter of high concern. Its reduction is of major public interest since it affects health and life of the community. This noise reduction is also of major industrial interest. Especially, nowadays combustion processes create acoustic sources of higher intensity in aircraft engines, which in their turn create acoustic instabilities around particular frequencies and may even harm the live time of the gas turbine. Engineers study liners, which are perforated wall segments, that are able to suppress thermo-acoustic instabilities and can provide a substantial amount of acoustic damping. An important type of acoustic liner for aero-engine inlet and exhaust ducts constitutes of a array of small cells called Helmholtz resonators. Each of the Helmholtz resonators – the name goes back to H. Helmholtz[19] consists of a rigid chamber filled with air that is connected to the surrounding by a hole of a perforated plate, that is called orifice or even neck. When excited with a fluctuating external pressure, that comes *e. g.*, from the combustion process, the mass of the air inside and around the orifice moves against the large volume of compressible air inside the cavity, while viscous effects cause dissipation of energy. This can be modeled as a mass-spring-damping system. The damping of this system is relatively small except for frequencies close to the resonance frequencies of the liner where it becomes considerably large. The resonance frequencies and damping properties depend mainly on the geometrical parameters of the resonators. For a small Helmholtz resonator the first resonance frequency – the Helmholtz resonance – can be approximated by a simple formula[19] of Helmholtz that has been justified by a mathematical analysis of the spectrum of the Laplace operator by Schweizer[49] as well as by an asymptotic analysis of the Green’s function of the Helmholtz equation[2]. It is based on the observation that the pressure is almost uniform inside the resonator and therefore the formula does not depend on the shape of the resonator, especially, if it is elongated or of compact size. The simple formula has been improved by a so-called end-correction[32, 24] of the aperture thickness. For elongated resonance chambers approximations of each resonance frequency can be obtained as solutions of a nonlinear equations using semi-analytical formulas for the behaviour of the pressure around the hole and in the chamber[36].

For an effective damping a large number of Helmholtz resonators are arrayed. Due to the high number of resonators and the involved smaller geometrical scales a direct numerical computations, *e. g.*, with the finite element method, would be not feasible. One is therefore interested in equivalent problems in the domain above the resonators and multiperforated plate. To predict the frequency dependent damping properties of

array of Helmholtz resonators impedance boundary conditions has been proposed that depend on one complex function of the frequency – the (normalized specified) acoustic impedance. First, such a semi-analytic formula for the impedance has been introduced by Guess[18] that depends again on the end-correction of the aperture thickness, to which nonlinear terms for high sound amplitudes can be added[25, 53] that are especially important close to resonance as well as terms in presence of a grazing flow[26, 43, 48]. The impedance of an array of Helmholtz resonators is also computed numerically by coupling the instationary viscous Navier-Stokes equations in frequency domain in some region around the orifice with the Euler equation away from it by Lidoine *et al.* [30]. A similar approach in time-domain on meshes refined close to the orifices is used in[54] where only close to the orifices viscosity is considered. However, it is not clear what is a good choice of the “viscous” region.

In this contribution, we present an asymptotic homogenization of an array of Helmholtz resonators of depth  $L$ , of small period  $\delta$  and of even smaller diameter of the orifices that is of the order  $\delta^2$  taking the viscosity scaled like  $\delta^4$  into account. In this way the respective dominant behaviour in three different geometric scales is considered. We derive impedance boundary conditions applying the method of two-scale convergence[35, 1] to the three different scales of the problem. To justify the weak convergence to the limit the stability estimate of the  $\delta$ -dependent problem has to be assumed. The impedance boundary conditions are expressed in terms of the *effective Rayleigh conductivity* of a perforated plate [46] (see [6, 5] for zero viscosity) and in terms of the reactance of the chambers that depends above all on their depths. The effective Rayleigh conductivity is the Rayleigh conductivity [38, 39] of one hole, which describes the ratio of the fluctuating volume flow through the hole to the driving pressure difference across the hole, divided by the area of one periodicity cell of the array. The effective Rayleigh conductivity depends on the geometrical parameters, especially, size and shape of the necks of the Helmholtz resonators and the distance between two resonators, as well as the physical parameters, especially the acoustic viscosities and the excitation frequency. Asymptotic homogenization for periodic transmission problems were performed for the Stokes equation with three scales[44], with two scales for the Helmholtz equation[8], using the periodic unfolding method[31] and the method of matched asymptotic expansion[14, 12], also with impedance boundary conditions in the holes[51]. Asymptotic homogenization for locally periodic transmission problems, where microstructures has finite size, and that takes the singular behaviour at the end of the microstructure into account, was derived and justified for the Laplace equation[34, 15] and the Helmholtz equation[50].

The article is subdivided as follows. In Sec. 2 we define the model problem of the viscous acoustic equations in terms of the acoustic velocity and pressure and the equivalent impedance boundary conditions on the array of resonators for the velocity and pressure. We also give as main result the weak convergence of the velocity and the pressure to their limits that fulfill a Helmholtz problem with the derived equivalent impedance boundary condition. For this result the assumption of an *a priori* stability result is needed that shall be proved in a forthcoming article. Sec. 3 is dedicated to the proof of the weak convergence to a limit using two-scale convergence step by step in different asymptotic regions where finally the limit model including impedance boundary conditions is obtained. Finally, in Sec. 4, the equivalent impedance boundary conditions are studied numerically and compared with the established model of Guess[18], both locally based on the reactance and resistance curves and resonance frequencies as well as macroscopically based on the dissipation behaviour of an array of Helmholtz resonators in a duct.

## 2 Description of the problem and main results

### 2.1 Description of the problem

We consider a three-dimensional domain  $\Omega$  that is open, simply connected and bounded with smooth boundary  $\partial\Omega$ . For the sake of simplicity we consider that  $\Omega$  is included in the half-space  $\mathbb{R}^2 \times \mathbb{R}_+$  such that its boundary  $\partial\Omega$  gives a non-empty intersection with the plane  $\{x_3 = 0\}$ .

We consider the surface  $\Gamma$  as a parallelepipedic subset of  $\partial\Omega \cap \{\mathbf{x} \in \mathbb{R}^3, x_3 = 0\}$ . We extend then the domain  $\Omega$  to a domain containing an array of Helmholtz resonators. We assume this array to be periodic, *i. e.*, there exists two fixed vectors  $\mathbf{a}_1$  and  $\mathbf{a}_2$  such that the centered parallelogram  $\mathcal{A}$  spanned by the vectors  $\mathbf{a}_1$  and  $\mathbf{a}_2$  is of area equal to 1, and there exists  $\delta > 0$  such that the set centers of apertures of resonators is given by (see Fig. 1a)

$$\Gamma^\delta := \Gamma \cap (\delta\mathbf{a}_1\mathbb{Z} + \delta\mathbf{a}_2\mathbb{Z}). \quad (2.1)$$

For simplicity, we assume that there exists  $L_1, L_2 > 0$  with  $L_1/L_2 \in \mathbb{Q}$  such that

$$\Gamma = \{\mathbf{x} = s_1\mathbf{a}_1 + s_2\mathbf{a}_2 \quad \text{with} \quad (s_1, s_2) \in (0, L_1) \times (0, L_2)\},$$

and  $\delta$  is chosen such that  $L_1/\delta$  and  $L_2/\delta$  are positive integers, *i. e.*, the number of Helmholtz resonators is equal to  $L_1L_2/\delta^2$ . To define the resonator chamber we introduce its cross section  $\mathcal{A}_C \subset \mathcal{A}$  that is a two-dimensional smooth open and simply-connected domain, and two constants  $d_0, h_0 > 0$ . For  $(n_1, n_2) \in \mathbb{Z}^2$  such that  $\mathbf{x}_\Gamma^\delta := \delta n_1\mathbf{a}_1 + \delta n_2\mathbf{a}_2 \in \Gamma^\delta$ , the resonator  $\Omega_H^\delta(\mathbf{x}_\Gamma^\delta)$  consists of a chamber part

$$\Omega_C^\delta(\mathbf{x}_\Gamma^\delta) := \mathbf{x}_\Gamma^\delta + \delta\mathcal{A}_C \times (-L, -\delta^2h_0), \quad (2.2)$$

and a neck part

$$\Omega_N^\delta(\mathbf{x}_\Gamma^\delta) := \mathbf{x}_\Gamma^\delta + \delta^2\Omega_N \quad (2.3)$$

with the bounded, open and simply connected Lipschitz domain  $\Omega_N \subset \mathbb{R}^2 \times (-h_0, 0)$  where  $0 \in \overline{\Omega_N}$  and the submanifolds  $\partial\Omega_N \cap \mathbb{R}^2 \times \{0\}$  and  $\partial\Omega_N \cap \mathbb{R}^2 \times \{-h_0\}$  are non-empty and smooth. Moreover, we consider  $\delta$  such that  $\delta(\partial\Omega_N \cap \mathbb{R}^2 \times \{-h_0\}) \subset \mathcal{A}_C \times \{-\delta h_0\}$ . A chamber and neck builds a resonator  $\Omega_H^\delta(\mathbf{x}_\Gamma^\delta) = \Omega_C^\delta(\mathbf{x}_\Gamma^\delta) \cup \Omega_N^\delta(\mathbf{x}_\Gamma^\delta)$ , and extending the domain  $\Omega$  by the union of all resonators we obtain the computational domain  $\Omega^\delta$  whose closure is defined by

$$\overline{\Omega^\delta} := \overline{\Omega} \cup \bigcup_{\mathbf{x}_\Gamma^\delta \in \Gamma^\delta} \overline{\Omega_H^\delta(\mathbf{x}_\Gamma^\delta)}. \quad (2.4)$$

On the domain  $\Omega^\delta$  we introduce the acoustic equations in the framework of Landau and Lifschitz[28] as a perturbation of the Navier-Stokes equations around a stagnant uniform fluid with mean density  $\rho_0$ .

We consider time-harmonic velocity  $\mathbf{v}^\delta$  and acoustic pressure  $p^\delta$  (the time regime is  $\exp(-i\omega t)$ ,  $\omega > 0$ ), which are solutions of the coupled system

$$-i\omega\mathbf{v}^\delta + \frac{1}{\rho_0}\nabla p^\delta - \nu(\delta)\Delta\mathbf{v}^\delta - \nu'(\delta)\nabla\operatorname{div}\mathbf{v}^\delta = \mathbf{f}, \quad \text{in } \Omega^\delta, \quad (2.5a)$$

$$-i\omega p^\delta + \rho_0 c^2 \operatorname{div}\mathbf{v}^\delta = 0, \quad \text{in } \Omega^\delta, \quad (2.5b)$$

$$\mathbf{v}^\delta = \mathbf{0}, \quad \text{on } \partial\Omega^\delta, \quad (2.5c)$$

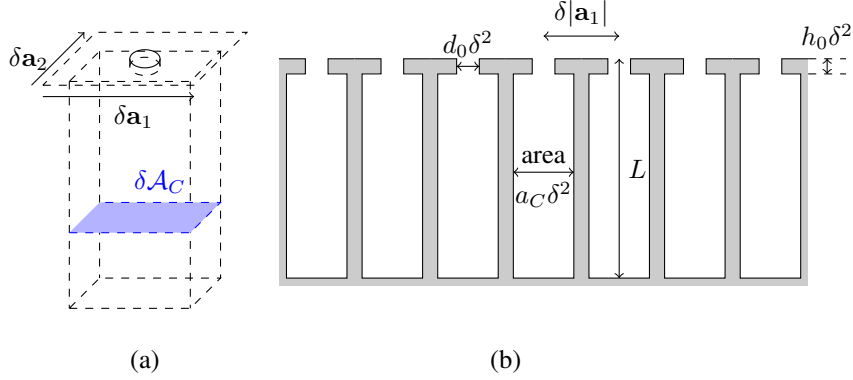


Figure 1: (a) Example of one resonator (square-shaped constant cross-sections) that connects through  $N_0 = 1$  hole. (b) Representation of the array of resonators (cut along one one periodicity direction).

with the speed of sound  $c$ , and the kinematic and secondary viscosities  $\nu(\delta), \nu'(\delta) > 0$  that we scale with the characteristic size of the holes  $\delta^2$  as

$$\nu(\delta) = \nu_0 \delta^4 \quad \text{and} \quad \nu'(\delta) = \nu'_0 \delta^4, \quad (2.6)$$

where  $\nu_0, \nu'_0$  are independent of  $\delta$ . In this way the thickness of the boundary layer of the acoustic velocity at the rigid wall[3, 4, 7, 23, 47] – that is of order  $O(\sqrt{\nu(\delta)})$  – is of the order of characteristic size of the holes  $\delta^2$  (see Fig. 1(b)). Moreover, the source term  $\mathbf{f}$  is independent of  $\delta$  and compactly supported in  $\Omega$  away from its boundary. Similar equations have been studied for a stagnant flow[22, 23, 28, 42] and for the case that a mean flow is present[4, 21, 22, 33, 41]. Finally, we embed the domain  $\Omega^\delta$  and the associate linear Navier-Stokes problem (2.5) in a family of problems that are  $\delta$ -dependent.

In the following, we define the effective Rayleigh conductivity of a single hole that will be used then to define impedance boundary conditions for the limit of  $(\mathbf{v}^\delta, p^\delta)$  for  $\delta \rightarrow 0$ .

## 2.2 Effective Rayleigh conductivity

To relate the pressure jump on different sides of a single hole to pressure and velocity profiles and eventually the flux through the hole we consider as characteristic problem an instantaneous Stokes system in scaled coordinates[46]: Seek  $(\mathbf{v}, \mathbf{p}) \in (H_0^1(\widehat{\Omega}))^3 \times L_{\text{loc}}^2(\widehat{\Omega})$  solution of

$$\begin{aligned} -i\omega \mathbf{v} + \frac{1}{\rho_0} \nabla \mathbf{p} - \nu_0 \Delta \mathbf{v} &= \mathbf{0}, & \text{in } \widehat{\Omega}, \\ \operatorname{div} \mathbf{v} &= 0, & \text{in } \widehat{\Omega}, \\ \mathbf{v} &= \mathbf{0}, & \text{on } \partial \widehat{\Omega}, \\ \lim_{S \rightarrow \infty} \mathbf{p}|_{\widehat{\Gamma}_\pm(S)} &= \pm \frac{1}{2}, \end{aligned} \quad (2.7)$$

with the family of surfaces

$$\begin{aligned}\widehat{\Gamma}_+(S) &:= \{\mathbf{z} \in \mathbb{R}^3 : |\mathbf{z}| = S, z_3 > 0\}, \\ \widehat{\Gamma}_-(S) &:= \{\mathbf{z} \in \mathbb{R}^3 : |\mathbf{z} - (0, 0, -h_0)| = S, z_3 < -h_0\}\end{aligned}$$

and the rescaled extended aperture domain  $\widehat{\Omega} := \cup_{S \in \mathbb{R}^+} \widehat{\Omega}(S)$  connecting two half-spaces (see Fig. 2(c) for illustration) where

$$\begin{aligned}\widehat{\Omega}(S) &:= \widehat{\Omega}_A \cup \{\mathbf{z} \in \mathbb{R}^3 : |\mathbf{z}| < S, z_3 > 0\} \\ &\cup \{\mathbf{z} \in \mathbb{R}^3 : |\mathbf{z} - (0, 0, -h_0)| < S, z_3 < -h_0\}.\end{aligned}$$

Due to the scaling all other holes are moved towards infinity and canonical problem considers the dominant phenomena on the scale of one hole, that is viscosity and incompressibility of the acoustic velocity that is with the acoustic pressure non-stationary.

The well-posedness of the characteristic problem is stated in the following

**Proposition 2.1.** *There exists a unique solution  $(\mathbf{v}, \mathbf{p}) \in (\mathbf{H}_0^1(\widehat{\Omega}))^3 \times L_{loc}^2(\widehat{\Omega})$  of (2.7).*

*Proof.* First we lift the condition for the pressure at infinity with a cut-off function

$$\Theta(\mathbf{z}) = \begin{cases} \frac{1}{2}, & z_3 > 0, \\ \frac{1}{2} + \frac{z_3}{h_0}, & 0 > z_3 > -h_0, \\ -\frac{1}{2}, & \text{otherwise} \end{cases}$$

We decompose then the pressure  $\mathbf{p}$  as  $\mathbf{p} = \Theta + \tilde{\mathbf{p}}$  and seek  $\tilde{\mathbf{p}}$  in the classical space  $L^2(\widehat{\Omega})$ . The variational formulation associated to (2.7) is: find  $(\mathbf{v}, \tilde{\mathbf{p}}) \in (\mathbf{H}_0^1(\widehat{\Omega}))^3 \times L^2(\widehat{\Omega})$  such that for any  $(\mathbf{w}, \mathbf{q}) \in (\mathbf{H}_0^1(\widehat{\Omega}))^3 \times L^2(\widehat{\Omega})$ ,

$$\begin{aligned}a(\mathbf{v}, \mathbf{w}) + b(\tilde{\mathbf{p}}, \mathbf{w}) &= \ell(\mathbf{w}), \\ b(\mathbf{q}, \mathbf{v}) &= 0,\end{aligned}\tag{2.8}$$

where the sesquilinear forms  $a$  and  $b$  are given by

$$a(\mathbf{v}, \mathbf{w}) := -i\omega \int_{\widehat{\Omega}} \mathbf{v} \cdot \overline{\mathbf{w}} \, d\mathbf{z} + \nu_0 \int_{\widehat{\Omega}} \nabla \mathbf{v} : \nabla \overline{\mathbf{w}} \, d\mathbf{z}, \quad b(\mathbf{q}, \mathbf{v}) := -\frac{1}{\rho_0} \int_{\widehat{\Omega}} \mathbf{q} \operatorname{div} \overline{\mathbf{v}} \, d\mathbf{z},$$

and the antilinear form  $\ell$  by

$$\ell(\mathbf{w}) := \frac{1}{\rho_0} \int_{\widehat{\Omega}} \nabla \Theta \cdot \overline{\mathbf{w}} \, d\mathbf{z}.$$

The formulation (2.8) has a saddle-point structure. The sesquilinear form  $a$  is continuous and elliptic on  $(\mathbf{H}_0^1(\widehat{\Omega}))^3$ . The sesquilinear form  $b$  defines a surjective operator  $B : (\mathbf{H}_0^1(\Omega))^3 \rightarrow L^2(\Omega)$  by

$$\langle B\mathbf{v}, \mathbf{q} \rangle_{\widehat{\Omega}} = b(\mathbf{q}, \mathbf{v}), \quad \forall (\mathbf{v}, \mathbf{q}) \in (\mathbf{H}_0^1(\Omega))^3 \times L^2(\Omega),$$

with closed range.

Following the theory of saddle-point problems[11] and in view of Theorem 1.1 of the works of Brezzi[10], problem (2.8) admits a unique solution  $(\mathbf{v}, \tilde{\mathbf{p}}) \in (\mathbf{H}_0^1(\widehat{\Omega}))^3 \times L^2(\widehat{\Omega})$ , and, hence, (2.7) has a unique solution.  $\square$

Following the formulation of the Rayleigh conductivity  $K_R$ [38, 39] which describes the ratio of the fluctuating volume flow to the driving pressure difference, we introduce the *effective Rayleigh conductivity*  $k_R$ [6, 46] as

$$k_R := \lim_{S \rightarrow \infty} \frac{i\omega\rho_0}{2} \left( \int_{\widehat{\Gamma}_+(S)} \mathbf{v} \cdot \mathbf{n} - \int_{\widehat{\Gamma}_-(S)} \mathbf{v} \cdot \mathbf{n} \right). \quad (2.9)$$

**Proposition 2.2.** *The above defined effective Rayleigh conductivity  $k_R$  is well defined, i. e., the integral of the normal flux of  $\mathbf{v}$  on  $\widehat{\Gamma}_\pm(S)$  tends to a finite, non-zero quantity as  $S$  tends to infinity. Moreover  $\operatorname{Re}(k_R) > 0$  and  $\operatorname{Im}(k_R) < 0$ .*

*Proof.* Taking the conjugate of (3.21a) leads to

$$i\omega\bar{\mathbf{v}} + \frac{1}{\rho_0}\nabla_{\mathbf{z}}\bar{p} - \nu_0\Delta_{\mathbf{z}}\bar{\mathbf{v}} = \mathbf{0}.$$

Multiplying this equation with  $\mathbf{v}$  and integrating over the domain  $\widehat{\Omega}(S)$  leads to

$$i\omega \|\mathbf{v}\|_{L^2(\widehat{\Omega}(S))}^2 + \frac{1}{\rho_0} \langle \nabla_{\mathbf{z}}\bar{p}, \mathbf{v} \rangle_{\widehat{\Omega}(S)} - \nu_0 \langle \Delta_{\mathbf{z}}\bar{\mathbf{v}}, \bar{\mathbf{v}} \rangle_{\widehat{\Omega}(S)} = 0. \quad (2.10)$$

Let us treat now the two scalar product terms using the Gauss' theorem. Using (3.21b) leads to

$$\langle \nabla_{\mathbf{z}}\bar{p}, \mathbf{v} \rangle_{\widehat{\Omega}(S)} = \langle \bar{p}, \mathbf{v} \cdot \mathbf{n} \rangle_{\partial\widehat{\Omega}(S)}$$

Using (3.21d) (which is also valid for the conjugate complex), the definition of the effective Rayleigh conductivity stated by (2.9) and the spherical harmonic decompositions of  $\bar{p}$  and  $\bar{\mathbf{v}}$  leads to

$$\lim_{S \rightarrow \infty} \langle \nabla_{\mathbf{z}}\bar{p}, \mathbf{v} \rangle_{\widehat{\Omega}(S)} = \frac{k_R}{i\omega\rho_0}$$

Similarly, the study of the  $L^2$ -scalar product between  $\Delta_{\mathbf{z}}\bar{\mathbf{v}}$  and  $\bar{\mathbf{v}}$  leads to

$$- \lim_{S \rightarrow \infty} \langle \Delta_{\mathbf{z}}\bar{\mathbf{v}}, \bar{\mathbf{v}} \rangle_{\widehat{\Omega}(S)} = \|\nabla\bar{\mathbf{v}}\|_{L^2(\widehat{\Omega})}^2$$

Taking then the limit in (2.10) as  $S \rightarrow \infty$  leads to

$$i\omega \|\mathbf{v}\|_{L^2(\widehat{\Omega}(S))}^2 + \nu_0 \|\nabla\bar{\mathbf{v}}\|_{L^2(\widehat{\Omega}(S))}^2 = -\frac{k_R}{i\omega\rho_0^2} = \frac{1}{\omega\rho_0^2} (-\operatorname{Im}(k_R) + i\operatorname{Re}(k_R))$$

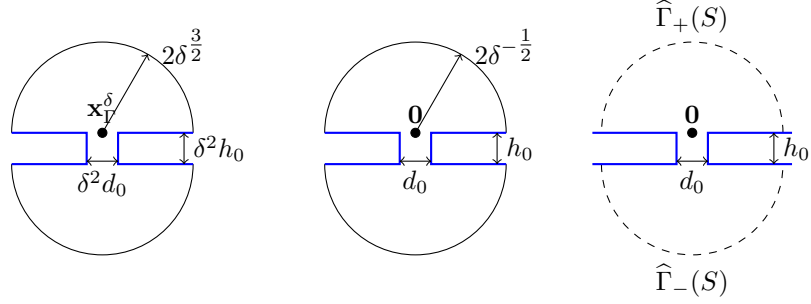
and therefore  $\operatorname{Re}(k_R) > 0$  and  $\operatorname{Im}(k_R) < 0$ .  $\square$

### 2.3 Weak convergence to a limit problem with impedance boundary conditions

As  $\delta$  tends to 0, we expect that the solution  $(\mathbf{v}^\delta, p^\delta)$  tends to a finite, non-trivial limit solution  $(\mathbf{v}_0, p_0)$  in the half-space  $\Omega$ , and we expect this limit term to be solution of an inviscid Helmholtz problem posed on  $\Omega$ .

**Definition 2.3** (Limit problem). *We define the limit problem  $(\mathbf{v}_0, p_0)$  as solution of*

$$\begin{aligned} -i\omega\mathbf{v}_0 + \frac{1}{\rho_0}\nabla p_0 &= \mathbf{f}, & \text{in } \Omega, \\ -i\omega p_0 + \rho_0 c^2 \operatorname{div} \mathbf{v}_0 &= 0, & \text{in } \Omega, \\ \left( \frac{ic\rho_0}{aC} \cos\left(\frac{\omega L}{c}\right) - \frac{i\omega\rho_0}{k_R} \sin\left(\frac{\omega L}{c}\right) \right) \mathbf{v}_0 \cdot \mathbf{n} - \sin\left(\frac{\omega L}{c}\right) p_0 &= 0, & \text{on } \Gamma, \\ \mathbf{v}_0 \cdot \mathbf{n} &= 0, & \text{on } \partial\Omega \setminus \Gamma. \end{aligned} \quad (2.11)$$



(a) Extended neck domain  $\Omega_A^\delta(\mathbf{x}_\Gamma^\delta)$  (b) Rescaled extended neck domain  $\widehat{\Omega}(2\delta^{-1/2})$  (c) Limit rescaled extended neck domain  $\widehat{\Omega}$

Figure 2: An extended neck domain in the original coordinates  $\mathbf{x}$  (left), in rescaled coordinates  $\mathbf{z} := \delta^{-2}(\mathbf{x} - \mathbf{x}_\Gamma^\delta)$  (middle) and the limit of the latter when  $\delta \rightarrow 0$  (right).

Note that, problem (2.11) is equivalent to a problem for the limit pressure  $p_0 \in H^1(\Omega)$  only, that is given by

$$\begin{aligned} \Delta p_0 + \frac{\omega^2}{c^2} p_0 &= \rho_0 \operatorname{div} \mathbf{f}, & \text{in } \Omega, \\ \left( \frac{c}{\omega a_C} \cos\left(\frac{\omega L}{c}\right) - \frac{1}{k_R} \sin\left(\frac{\omega L}{c}\right) \right) \nabla p_0 \cdot \mathbf{n} - \sin\left(\frac{\omega L}{c}\right) p_0 &= 0, & \text{on } \Gamma, \\ \nabla p_0 \cdot \mathbf{n} &= 0, & \text{on } \partial\Omega \setminus \Gamma, \end{aligned} \quad (2.12)$$

where  $\mathbf{v}_0 := \frac{i}{\omega} (\mathbf{f} - \frac{1}{\rho_0} \nabla p_0)$  follows. It is also equivalent to a problem for the limit velocity  $\mathbf{v}_0 \in H(\operatorname{div}, \Omega) \cap H(\operatorname{curl}, \Omega)$  only that is

$$\begin{aligned} \nabla \operatorname{div} \mathbf{v}_0 + \frac{\omega^2}{c^2} \mathbf{v}_0 &= \frac{i\omega}{c^2} \mathbf{f}, & \text{in } \Omega, \\ \operatorname{curl} \mathbf{v}_0 &= -\frac{1}{i\omega} \operatorname{curl} \mathbf{f}, & \text{in } \Omega, \\ \left( \frac{c}{\omega a_C} \cos\left(\frac{\omega L}{c}\right) - \frac{1}{k_R} \sin\left(\frac{\omega L}{c}\right) \right) \mathbf{v}_0 \cdot \mathbf{n} & & (2.13) \\ - \left( \frac{c^2}{\omega^2} \sin\left(\frac{\omega L}{c}\right) \right) \operatorname{div} \mathbf{v}_0 &= 0, & \text{on } \Gamma, \\ \mathbf{v}_0 \cdot \mathbf{n} &= 0, & \text{on } \partial\Omega \setminus \Gamma, \end{aligned}$$

where  $p_0 := \frac{-i\rho_0 c^2}{\omega} \operatorname{div} \mathbf{v}_0$  follows.

The nature of the boundary condition on  $\Gamma$  depends on the value of  $\sin \frac{\omega L}{c}$

1. If  $\sin\left(\frac{\omega L}{c}\right) = 0$ , *i.e.*, if  $\frac{\omega}{c}$  corresponds to a characteristic wavelength of the one-dimensional Helmholtz problem in a domain of size  $L$ , then the boundary condition on  $\Gamma$  becomes  $\mathbf{v}_0 \cdot \mathbf{e}_3 = 0$ , therefore  $\mathbf{v}_0 \cdot \mathbf{n} = 0$  on the whole boundary  $\partial\Omega$ .
2. *A contrario*, if  $\sin\left(\frac{\omega L}{c}\right) \neq 0$ , the right-hand side does not vanish, and denoting here by  $\mathbf{n} := -\mathbf{e}_3$  the unit outward normal vector on  $\Gamma$ , one gets the impedance condition

$$\left( -\frac{ic}{a_C(\mathbf{x}_\Gamma)} \cot\left(\frac{\omega L}{c}\right) + \frac{i\omega}{k_R(\mathbf{x}_\Gamma)} \right) \mathbf{v}_0(\mathbf{x}_\Gamma) \cdot \mathbf{n} + \frac{1}{\rho_0} p_0(\mathbf{x}_\Gamma) = 0, \quad (2.14)$$

and this equation gives an acoustic impedance  $Z(\omega)$  of the same nature as the one derived by Rienstra and Singh[43, Eq. (14)].



We give the existence and uniqueness result of the limit problem:

**Lemma 2.4** (Existence and uniqueness of the limit problem). *Let  $\mathbf{f} \in \mathbf{H}(\operatorname{div}, \Omega)$ . Then, the limit problem (2.11) is well-posed, i. e., admits a unique solution  $(\mathbf{v}_0, p_0) \in \mathbf{H}(\operatorname{div}, \Omega) \times \mathbf{H}^1(\Omega)$ , except for frequencies  $\omega \in \Lambda$ , where  $\Lambda$  is a subset of  $\frac{\pi c}{L}\mathbb{N}$ .*

This lemma will be proved later in Section 3.6.

We give now the main theoretical result of this paper.

**Theorem 2.5** (Weak convergence to the limit problem). *Let  $\omega \notin \Lambda$  with the set  $\Lambda$  in Lemma 2.4,  $\mathbf{f} \in \mathbf{H}(\operatorname{div}, \Omega)$  and there exist two constants  $C_\Omega > 0$  and  $\delta_0 > 0$  such that for all  $\delta \in (0, \delta_0)$  it holds for the solution  $(\mathbf{v}^\delta, p^\delta)$  of (2.5)*

$$\|\mathbf{v}^\delta\|_{\mathbf{H}(\operatorname{div}, \Omega^\delta)} + \delta^2 \|\operatorname{curl} \mathbf{v}^\delta\|_{\mathbf{L}^2(\Omega^\delta)^3} + \|p^\delta\|_{\mathbf{H}^1(\Omega^\delta)} \leq C_\Omega. \quad (2.15)$$

Then  $(\mathbf{v}^\delta, p^\delta)$  converges weakly in  $\mathbf{H}(\operatorname{div}, \Omega) \times \mathbf{H}^1(\Omega)$  to the solution  $(\mathbf{v}_0, p_0)$  of (2.11).

In a forthcoming article we shall prove the estimate (2.15).

**Remark 2.6.** *The following study is done on a flat interface  $\Gamma$  for simplicity. For slow varying interfaces, the upcoming limit model can be derived using an appropriate variable change that flattens the surface. For the example of a cylindrical array of Helmholtz resonators, as it can be seen on Fig. 3, such a variable change has been used in a previous work[46].*

### 3 Proof of the weak convergence to the limit

In this section, we derive the limit problem (2.11) on  $\Omega$  using the two-scale convergence. To do so, we show that, up to a subsequence,  $(\mathbf{v}^\delta, p^\delta)$  converges weakly in  $\mathbf{H}(\operatorname{div}, \Omega) \times \mathbf{H}^1(\Omega)$  to a limit  $(\mathbf{v}_0, p_0)$  that satisfies an Helmholtz- $\nabla \operatorname{div}$  equation with radiation conditions. To obtain this result we prove the weak convergence of  $\mathbf{v}^\delta$  in each subpart of  $\Omega^\delta$ , i. e., the domain  $\Omega$  not including the interface  $\Gamma$ , the array of resonator chambers, the two-semi infinite strips of the pattern  $\mathcal{B}^\delta$  and the array of resonator apertures, where matching conditions and finally impedance conditions follow.

From this stability result, we derive another *a priori* error estimate on what we will call the *extended Helmholtz resonator array*. We first extend the Helmholtz resonator

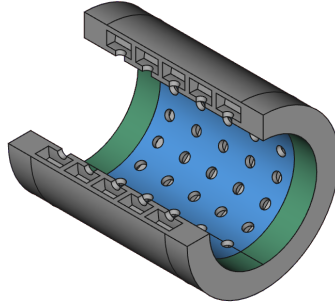


Figure 3: A cylindrical liner for which in the limit  $\delta \rightarrow 0$  the same impedance boundary conditions appear as for the considered flat surface.

$\Omega_H^\delta(\mathbf{x}_\Gamma^\delta)$  centered at  $\mathbf{x}_\Gamma^\delta$  into an *extended Helmholtz resonator*  $\tilde{\Omega}_H^\delta(\mathbf{x}_\Gamma^\delta)$  defined as

$$\tilde{\Omega}_H^\delta(\mathbf{x}_\Gamma^\delta) = \Omega_H^\delta(\mathbf{x}_\Gamma^\delta) \cup (\mathbf{x}_\Gamma^\delta + \mathcal{A} \times (0, 2\sqrt{\delta})).$$

**Lemma 3.1.** *Let  $\omega \notin \Lambda$ , and let the assumption estimate (2.15) holds. There exists two constants  $C_H > 0$  and  $\delta_0 > 0$  such that, for any  $\delta \in (0, \delta_0)$ , the estimate*

$$\begin{aligned} \sum_{\mathbf{x}_\Gamma^\delta \in \Gamma^\delta} \|\mathbf{v}^\delta\|_{\mathbf{H}(\text{div}, \tilde{\Omega}_H^\delta(\mathbf{x}_\Gamma^\delta))}^2 + \sum_{\mathbf{x}_\Gamma^\delta \in \Gamma^\delta} \delta^2 \|\mathbf{curl} \mathbf{v}^\delta\|_{\mathbf{L}^2(\tilde{\Omega}_H^\delta(\mathbf{x}_\Gamma^\delta))}^2 \\ + \sum_{\mathbf{x}_\Gamma^\delta \in \Gamma^\delta} \|p^\delta\|_{\mathbf{H}^1(\tilde{\Omega}_H^\delta(\mathbf{x}_\Gamma^\delta))}^2 \leq C_H. \end{aligned} \quad (3.1)$$

holds.

*Proof.* Let  $\omega \notin \Lambda$ , and let the assumption estimate (2.15) holds. Taking the square of this estimate, and using that the union of all  $\tilde{\Omega}_H^\delta(\mathbf{x}_\Gamma^\delta)$  over  $\mathbf{x}_\Gamma^\delta$  is a subset of  $\Omega^\delta$  leads to estimate (3.1) with  $C_H = 3C_\Omega^2$ .  $\square$

In the following, we use the estimate of this Lemma in each subsection: the array of Helmholtz resonators, the array of patterns below apertures, the array of apertures and the array of patterns above apertures.

### 3.1 Weak convergence in the resonator array

In this section, we consider for each  $\delta > 0$ ,  $\mathbf{x} = (x_1, x_2, x_3) \in \Omega^\delta$  with  $x_3 < -\sqrt{\delta}$ . At the first glance, we have to study positions  $\mathbf{x}$  depending on  $\delta$ , since the location of each Helmholtz resonator depends on  $\delta$ . However, later we will see how to separate these dependencies.

Due to the geometrical assumption on the array of Helmholtz resonators, for each  $\mathbf{x}$  in the array of Helmholtz resonators, there exists a center of aperture of one resonator, which we call resonator position  $\mathbf{x}_\Gamma^\delta \in \Gamma^\delta$  such that  $\mathbf{x} \in \Omega_C^\delta(\mathbf{x}_\Gamma^\delta)$ . We introduce the two-dimensional point  $\mathbf{y} \in \mathcal{A}_C$ , that we identify with abuse of notation to the three-dimensional point  $(\mathbf{y}, 0)$ , such that

$$\mathbf{x} \mapsto (\mathbf{y}, x_3) := \left(\frac{1}{\delta}(\mathbf{x} - \mathbf{x}_\Gamma^\delta), x_3\right) \in \mathcal{A}_C \times (-L, -\sqrt{\delta}),$$

*i. e.*,  $\mathbf{x} = \mathbf{x}_\Gamma^\delta + (0, 0, x_3) + \delta\mathbf{y}$ . Using the coordinate  $(\mathbf{y}, x_3)$  means to stretch the resonator  $\Omega_H^\delta(\mathbf{x}_\Gamma^\delta)$  in the transverse plane  $(\mathbf{e}_1, \mathbf{e}_2)$ , and in this plane only. The stretched resonator chamber is denoted by  $\tilde{\Omega}_C^\delta := \mathcal{A}_C \times (-L, -\sqrt{\delta})$ .

In the following, we introduce the five-dimensional functions  $\mathbf{V}^\delta$  and  $P^\delta$ , depending on the resonator position  $\mathbf{x}_\Gamma^\delta$ , the slow longitudinal variable  $x_3$  and the fast transverse variable  $\mathbf{y}$ , by

$$\begin{aligned} \mathbf{V}^\delta(\mathbf{x}_\Gamma^\delta, x_3, \mathbf{y}) &= \mathbf{v}^\delta(\mathbf{x}_\Gamma^\delta + (0, 0, x_3) + \delta\mathbf{y}), \\ P^\delta(\mathbf{x}_\Gamma^\delta, x_3, \mathbf{y}) &= p^\delta(\mathbf{x}_\Gamma^\delta + (0, 0, x_3) + \delta\mathbf{y}). \end{aligned} \quad (3.2)$$

Considering the linearized Navier-Stokes problem (2.5) with the Laplace operator written as  $\Delta = \nabla \text{div} - \mathbf{curl} \mathbf{curl}$  and applying the anisotropic coordinate change, we

obtain the system

$$-i\omega \mathbf{V}^\delta + \frac{1}{\delta\rho_0} \nabla_{\mathbf{y}} P^\delta + \frac{1}{\rho_0} \partial_{x_3} P^\delta \mathbf{e}_3 \quad (3.3a)$$

$$\begin{aligned} & -(\nu_0 + \nu'_0) \delta^2 \nabla_{\mathbf{y}} \operatorname{div}_{\mathbf{y}} \mathbf{V}^\delta \\ & -(\nu_0 + \nu'_0) \delta^2 \partial_{\mathbf{e}_3} \operatorname{div}_{\mathbf{y}} \mathbf{V}^\delta \mathbf{e}_3 - \\ & (\nu_0 + \nu'_0) \delta^3 \nabla_{\mathbf{y}} (\partial_{x_3} \mathbf{V}^\delta \cdot \mathbf{e}_3) \\ & -(\nu_0 + \nu'_0) \delta^4 \partial_{x_3} (\partial_{x_3} \mathbf{V}^\delta \cdot \mathbf{e}_3) \\ & + \nu_0 \delta^4 \left( \frac{1}{\delta} \partial_{y_1}, \frac{1}{\delta} \partial_{y_2}, \partial_{x_3} \right) \wedge \left( \left( \frac{1}{\delta} \partial_{y_1}, \frac{1}{\delta} \partial_{y_2}, \partial_{x_3} \right) \wedge \mathbf{V}^\delta \right) = \mathbf{0}, \quad \text{in } \Gamma^\delta \times \widehat{\Omega}_C^\delta, \\ & -i\omega P^\delta + \frac{\rho_0 c^2}{\delta} \operatorname{div}_{\mathbf{y}} \mathbf{V}^\delta + \rho_0 c^2 (\partial_{x_3} \mathbf{V}^\delta \cdot \mathbf{e}_3) = 0, \quad \text{in } \Gamma^\delta \times \widehat{\Omega}_C^\delta, \end{aligned} \quad (3.3b)$$

$$\mathbf{V}^\delta = \mathbf{0}, \quad \text{on } \Gamma^\delta \times (-L, -\sqrt{\delta}) \times \partial \mathcal{A}_C, \quad (3.3c)$$

$$\mathbf{V}^\delta = \mathbf{0}, \quad \text{on } \Gamma^\delta \times \{-L\} \times \mathcal{A}_C. \quad (3.3d)$$

The estimate (3.1) of the Lemma 3.1 is equivalent to state in rescaled coordinates that

$$\begin{aligned} & \sum_{\mathbf{x}_\Gamma^\delta \in \Gamma^\delta} \|\mathbf{V}^\delta(\mathbf{x}_\Gamma^\delta, \cdot)\|_{L^2(\widehat{\Omega}_C^\delta)}^2 + \frac{1}{\delta^2} \sum_{\mathbf{x}_\Gamma^\delta \in \Gamma^\delta} \|\operatorname{div}_{\mathbf{y}} \mathbf{V}^\delta\|_{L^2(\widehat{\Omega}_C^\delta)}^2 \\ & + \sum_{\mathbf{x}_\Gamma^\delta \in \Gamma^\delta} \|\partial_{x_3} \mathbf{V}^\delta(\mathbf{x}_\Gamma^\delta, \cdot) \cdot \mathbf{e}_3\|_{L^2(\widehat{\Omega}_C^\delta)}^2 + \delta^4 \sum_{\mathbf{x}_\Gamma^\delta \in \Gamma^\delta} \left\| \left( \frac{1}{\delta} \partial_{y_1}, \frac{1}{\delta} \partial_{y_2}, \partial_{x_3} \right) \wedge \mathbf{V}^\delta(\mathbf{x}_\Gamma^\delta, \cdot) \right\|_{L^2(\widehat{\Omega}_C^\delta)}^2 \\ & + \sum_{\mathbf{x}_\Gamma^\delta \in \Gamma^\delta} \|P^\delta(\mathbf{x}_\Gamma^\delta, \cdot)\|_{L^2(\widehat{\Omega}_C^\delta)}^2 + \frac{1}{\delta^2} \sum_{\mathbf{x}_\Gamma^\delta \in \Gamma^\delta} \|\nabla_{\mathbf{y}} P^\delta(\mathbf{x}_\Gamma^\delta, \cdot)\|_{L^2(\widehat{\Omega}_H^\delta(\mathbf{x}_\Gamma^\delta))}^2 \\ & + \sum_{\mathbf{x}_\Gamma^\delta \in \Gamma^\delta} \|\partial_{x_3} P^\delta(\mathbf{x}_\Gamma^\delta, \cdot)\|_{L^2(\widehat{\Omega}_C^\delta)}^2 \leq C_H. \end{aligned} \quad (3.4)$$

The main idea is to extend the functions  $(\mathbf{V}^\delta, P^\delta)$  *discrete* with respect to  $\mathbf{x}_\Gamma^\delta \in \Gamma^\delta$  to functions still denoted by  $(\mathbf{V}^\delta, P^\delta)$  and *continuous* with respect to  $\mathbf{x} \in \Gamma$  by the following

$$(\mathbf{V}^\delta, P^\delta)(\mathbf{x}_\Gamma, \cdot) = (\mathbf{V}^\delta, P^\delta)(\mathbf{x}_\Gamma^\delta, \cdot), \quad \mathbf{x}_\Gamma \in \mathbf{x}_\Gamma^\delta + \delta \mathcal{A}.$$

The equation (3.3) is then extended naturally on  $\mathbf{x}_\Gamma \in \Gamma$  (the parameter  $\mathbf{x}_\Gamma^\delta$  is only playing a parameter), and the *discrete* error estimate (3.4) is extended to a *continuous* error estimate

$$\begin{aligned} & \|\mathbf{V}^\delta\|_{L^2(\Gamma; L^2(\widehat{\Omega}_C^\delta))}^2 + \frac{1}{\delta^2} \|\operatorname{div}_{\mathbf{y}} \mathbf{V}^\delta\|_{L^2(\Gamma; L^2(\widehat{\Omega}_C^\delta))}^2 + \|\partial_{x_3} \mathbf{V}^\delta \cdot \mathbf{e}_3\|_{L^2(\Gamma; L^2(\widehat{\Omega}_C^\delta))}^2 \\ & + \delta^4 \left\| \left( \frac{1}{\delta} \partial_{y_1}, \frac{1}{\delta} \partial_{y_2}, \partial_{x_3} \right) \wedge \mathbf{V}^\delta \right\|_{L^2(\Gamma; L^2(\widehat{\Omega}_C^\delta))}^2 + \|P^\delta\|_{L^2(\Gamma; L^2(\widehat{\Omega}_C^\delta))}^2 \\ & + \frac{1}{\delta^2} \|\nabla_{\mathbf{y}} P^\delta\|_{L^2(\Gamma; L^2(\widehat{\Omega}_C^\delta))}^2 + \|\partial_{x_3} P^\delta\|_{L^2(\Gamma; L^2(\widehat{\Omega}_C^\delta))}^2 \leq C_H |\mathcal{A}|. \end{aligned} \quad (3.5)$$

This means that the sequence  $(\mathbf{V}^\delta, P^\delta)$  is bounded in  $L^2(\Gamma; \mathbf{H}(\operatorname{div}, \widehat{\Omega}_C^\delta)) \times L^2(\Gamma; \mathbf{H}^1(\widehat{\Omega}_C^\delta))$ , independent of  $\delta \rightarrow 0$  even the domain  $\widehat{\Omega}_C^\delta$  enlarges for decreasing  $\delta$ . Then, for any fixed  $\varepsilon > 0$  and for any  $\delta < \varepsilon$ , the sequence  $(\mathbf{V}^\delta, P^\delta)$  is bounded in  $L^2(\Gamma; \mathbf{H}(\operatorname{div}, \widehat{\Omega}_C^\varepsilon)) \times L^2(\Gamma; \mathbf{H}^1(\widehat{\Omega}_C^\varepsilon))$  therefore we can extract a subsequence that we still denote by  $(\mathbf{V}^\delta, P^\delta)$  that converges to a limit  $(\mathbf{V}_0^\varepsilon, P_0^\varepsilon)$  weakly in  $L^2(\Gamma; \mathbf{H}(\operatorname{div}, \widehat{\Omega}_C^\varepsilon)) \times L^2(\Gamma; \mathbf{H}^1(\widehat{\Omega}_C^\varepsilon))$ .

Combining the lower semi-continuity of the weak limit stated by the Theorem 2.2.1 of the book of Evans[16] with the estimate (3.5), we find

$$\|\nabla_{\mathbf{y}} P_0^\varepsilon\|_{L^2(\Gamma; L^2(\widehat{\Omega}_C^\varepsilon)^2)} \leq \liminf_{\delta \rightarrow 0} \|\nabla_{\mathbf{y}} P^\delta\|_{L^2(\Gamma; L^2(\widehat{\Omega}_C^\delta)^2)} \leq \liminf_{\delta \rightarrow 0} \delta \sqrt{C_H |\mathcal{A}|} = 0.$$

This motivates us to take the scalar product of (3.3) with test functions  $(\mathbf{W}, Q)$  with  $Q$  independent of the fast transverse variable  $\mathbf{y}$ . Then, integrating by parts equation (3.3) leads to

$$\begin{aligned} & -i\omega \langle \mathbf{V}^\delta(\mathbf{x}_\Gamma, \cdot), \mathbf{W} \rangle_{(\widehat{\Omega}_C^\varepsilon)^3} + \frac{1}{\rho_0} \langle \partial_{x_3} P^\delta(\mathbf{x}_\Gamma, \cdot) \mathbf{e}_3, \mathbf{W} \rangle_{(\widehat{\Omega}_C^\varepsilon)^3} \\ & - \nu_0 \delta^4 \langle (\frac{1}{\delta} \partial_{y_1}, \frac{1}{\delta} \partial_{y_2}, \partial_{x_3}) \wedge \mathbf{V}^\delta(\mathbf{x}_\Gamma, \cdot), (0, 0, \partial_{x_3}) \wedge \mathbf{W} \rangle_{(\widehat{\Omega}_C^\varepsilon)^3} \\ & + (\nu_0 + \nu'_0) \delta^2 \langle \operatorname{div}_{\mathbf{y}}(\mathbf{x}_\Gamma, \cdot) \mathbf{V}^\delta, \operatorname{div}_{\mathbf{y}} \mathbf{W} \cdot \mathbf{e}_3 \rangle_{\widehat{\Omega}_C^\varepsilon} \\ & + (\nu_0 + \nu'_0) \delta^3 \langle \partial_{x_3}(\mathbf{x}_\Gamma, \cdot) \mathbf{V}^\delta, \operatorname{div}_{\mathbf{y}} \mathbf{W} \cdot \mathbf{e}_3 \rangle_{\widehat{\Omega}_C^\varepsilon} \\ & + (\nu_0 + \nu'_0) \delta^3 \langle \operatorname{div}_{\mathbf{y}}(\mathbf{x}_\Gamma, \cdot) \mathbf{V}^\delta, \partial_{x_3} \mathbf{W} \cdot \mathbf{e}_3 \rangle_{\widehat{\Omega}_C^\varepsilon} \\ & + (\nu_0 + \nu'_0) \delta^4 \langle \partial_{x_3} \mathbf{V}^\delta(\mathbf{x}_\Gamma, \cdot) \cdot \mathbf{e}_3, \partial_{x_3} \mathbf{W} \cdot \mathbf{e}_3 \rangle_{\widehat{\Omega}_C^\varepsilon} = 0, \\ & -i\omega \langle P^\delta(\mathbf{x}_\Gamma, \cdot), Q \rangle_{\widehat{\Omega}_C^\varepsilon} + \rho_0 c^2 \langle \nabla_{\mathbf{y}} \mathbf{V}^\delta(\mathbf{x}_\Gamma, \cdot), Q \rangle_{\widehat{\Omega}_C^\varepsilon} \\ & + \rho_0 c^2 \langle \partial_{x_3} \mathbf{V}^\delta(\mathbf{x}_\Gamma, \cdot) \cdot \mathbf{e}_3, Q \rangle_{\widehat{\Omega}_C^\varepsilon} = 0. \end{aligned} \quad (3.6)$$

Then, using the weak convergence of  $(\mathbf{V}^\delta, P^\delta)$  to  $(\mathbf{V}_0^\varepsilon, P_0^\varepsilon)$  in  $L^2(\Gamma; \mathbf{H}(\operatorname{div}, \widehat{\Omega}_C^\varepsilon)) \times L^2(\Gamma; \mathbf{H}^1(\widehat{\Omega}_C^\varepsilon))$  using estimate (3.5), we find the limit  $\delta \rightarrow 0$  for almost all  $\mathbf{x}_\Gamma \in \Gamma$

$$-i\omega \langle \mathbf{V}_0^\varepsilon(\mathbf{x}_\Gamma, \cdot), \mathbf{W} \rangle_{(\widehat{\Omega}_C^\varepsilon)^3} + \frac{1}{\rho_0} \langle \partial_{x_3} P_0^\varepsilon(\mathbf{x}_\Gamma, \cdot) \mathbf{e}_3, \mathbf{W} \rangle_{(\widehat{\Omega}_C^\varepsilon)^3} = 0, \quad (3.7a)$$

$$-i\omega \langle P_0^\varepsilon(\mathbf{x}_\Gamma, \cdot), Q \rangle_{\widehat{\Omega}_C^\varepsilon} + \rho_0 c^2 \langle \partial_{x_3} \mathbf{V}_0^\varepsilon(\mathbf{x}_\Gamma, \cdot) \cdot \mathbf{e}_3, Q \rangle_{\widehat{\Omega}_C^\varepsilon} = 0. \quad (3.7b)$$

The arbitrary choice of  $\mathbf{W}$  leads to

$$-i\omega \mathbf{V}_0^\varepsilon(\mathbf{x}_\Gamma, \cdot) + \frac{1}{\rho_0} \partial_{x_3} P_0^\varepsilon(\mathbf{x}_\Gamma, \cdot) \mathbf{e}_3 = 0,$$

and gives *a posteriori* that  $\mathbf{V}_0^\varepsilon(\mathbf{x}_\Gamma, \cdot)$  is also independent of  $\mathbf{y}$  and is directed among the  $\mathbf{e}_3$  direction, *i. e.*, there exists a scalar function  $V_{0,3}^\varepsilon$  independent of  $\mathbf{y}$  such that

$$\mathbf{V}_0^\varepsilon(\mathbf{x}_\Gamma, x_3, \mathbf{y}) = V_{0,3}^\varepsilon(\mathbf{x}_\Gamma, x_3) \mathbf{e}_3.$$

Taking then the equation (3.7b), we deduce that

$$-i\omega P_0^\varepsilon(\mathbf{x}_\Gamma, \cdot) + \rho_0 c^2 \partial_{x_3} \mathbf{V}_0^\varepsilon(\mathbf{x}_\Gamma, \cdot) \cdot \mathbf{e}_3 = 0,$$

*i. e.*, that  $(\mathbf{V}_0^\varepsilon(\mathbf{x}_\Gamma, \cdot), P_0^\varepsilon(\mathbf{x}_\Gamma, \cdot))$  is solution of an homogeneous one-dimensional Helmholtz equation. Derivation of the boundary condition at  $x_3 = -L$  is done as follow: we take a particular test function  $W$  depending on  $(x_3, \mathbf{y}) \in (-L, 0) \times \mathcal{A}_C$  such that  $W(x_3, \mathbf{y}) = 1$  for  $x_3 < -3L/4$  and  $W(x_3, \mathbf{y}) = 0$  for  $x_3 > -L/2$ , and using a one-dimensional Stokes formula coupled to the weak convergence of  $\mathbf{V}^\delta$  to  $V_{0,3}^\varepsilon \mathbf{e}_3$  in  $(L^2(\Gamma; L^2(\widehat{\Omega}_C^\delta)))$  gives

$$\begin{aligned} 0 &= \lim_{\delta \rightarrow 0} \int_{\mathcal{A}_C} \left\{ \partial_{x_3} (\mathbf{V}^\delta(\mathbf{x}_\Gamma, x_3, \mathbf{y}) \cdot \mathbf{e}_3 - V_{0,3}^\varepsilon(\mathbf{x}_\Gamma, x_3)) W(x_3) \right. \\ & \left. + (\mathbf{V}^\delta(\mathbf{x}_\Gamma, x_3, \mathbf{y}) \cdot \mathbf{e}_3 - V_{0,3}^\varepsilon(\mathbf{x}_\Gamma, x_3)) \partial_{x_3} W(x_3) \right\} d\mathbf{y} dx_3 = -a_C V_{0,3}^\varepsilon(\mathbf{x}_\Gamma, x_3), \end{aligned}$$

so there exists a scalar function  $V_0^\varepsilon$  depending only on the resonator position such that

$$\begin{aligned}\mathbf{V}_0^\varepsilon(\mathbf{x}_\Gamma, x_3) &= V_0^\varepsilon(\mathbf{x}_\Gamma) \sin\left(\frac{\omega}{c}(L + x_3)\right) \\ P_0^\varepsilon(\mathbf{x}_\Gamma, x_3) &= -i\rho_0 c V_0^\varepsilon(\mathbf{x}_\Gamma) \cos\left(\frac{\omega}{c}(L + x_3)\right).\end{aligned}\quad (3.8)$$

The next point is to derive a limit problem on the domain  $\widehat{\Omega}_C := \lim_{\varepsilon \rightarrow 0} \widehat{\Omega}_C^\varepsilon = \mathcal{A}_C \times (-L, 0)$ . To do so, using the lower semi-continuity of the weak limit  $(\mathbf{V}_0^\varepsilon, P_0^\varepsilon)$  with the *a priori* estimate (3.5), it holds

$$\begin{aligned}\|\mathbf{V}_0^\varepsilon\|_{L^2(\Gamma, L^2(\widehat{\Omega}_C^\varepsilon))}^2 + \|\partial_{x_3} \mathbf{V}_0^\varepsilon\|_{L^2(\Gamma, L^2(\widehat{\Omega}_C^\varepsilon))}^2 \\ + \|P_0^\varepsilon\|_{L^2(\Gamma, L^2(\widehat{\Omega}_C^\varepsilon))}^2 + \|\partial_{x_3} P_0^\varepsilon\|_{L^2(\Gamma, L^2(\widehat{\Omega}_C^\varepsilon))}^2 \leq C_H |\mathcal{A}|.\end{aligned}$$

This error estimate combined to (3.8) leads to

$$\left(1 + \frac{\omega^2}{c^2} + \rho_0^2 c^2 + \rho_0^2 \omega^2\right) (L - \sqrt{\varepsilon}) \|V_0^\varepsilon\|_{L^2(\Gamma)}^2 \leq 2C_H |\mathcal{A}|.$$

Extending  $(\mathbf{V}_0^\varepsilon, P_0^\varepsilon)$  on  $\mathcal{A} \times (-L, 0)$  using formula (3.8) and using this last error estimate leads to, for  $2\sqrt{\varepsilon} < L$ ,

$$\begin{aligned}\|\mathbf{V}_0^\varepsilon\|_{L^2(\Gamma, L^2(\widehat{\Omega}_C^0))}^2 + \|\partial_{x_3} \mathbf{V}_0^\varepsilon\|_{L^2(\Gamma, L^2(\widehat{\Omega}_C^0))}^2 \\ + \|P_0^\varepsilon\|_{L^2(\Gamma, L^2(\widehat{\Omega}_C^0))}^2 + \|\partial_{x_3} P_0^\varepsilon\|_{L^2(\Gamma, L^2(\widehat{\Omega}_C^0))}^2 \leq \frac{2L}{L - \sqrt{\varepsilon}} C_H |\mathcal{A}| \leq 4C_H |\mathcal{A}|.\end{aligned}$$

so that  $(\mathbf{V}_0^\varepsilon, P_0^\varepsilon)$  is uniformly bounded in  $L^2(\Gamma; \mathbf{H}(\text{div}; \widehat{\Omega}_C) \times \mathbf{H}^1(\widehat{\Omega}_C))$ . There exists then a subsequence that we still denote by  $(\mathbf{V}_0^\varepsilon, P_0^\varepsilon)$  that weakly converges to a limit  $(\mathbf{V}_0, P_0) \in L^2(\Gamma; \mathbf{H}(\text{div}; \widehat{\Omega}_C) \times \mathbf{H}^1(\widehat{\Omega}_C))$ .

We have two small quantities,  $\delta$  and  $\varepsilon$ , and we want to make these two quantities tending to 0. To do so, we will make a diagonal construction of  $(\mathbf{V}^\delta, P^\delta)$  to  $(V_{0,3} \mathbf{e}_3, P_0)$  by the following

1.  $(\mathbf{V}^\delta, P^\delta)$  is bounded in  $L^2(\Gamma; (\mathbf{H}(\text{div}; \widehat{\Omega}_C^{\varepsilon_1}))^3 \times \mathbf{H}^1(\widehat{\Omega}_C^{\varepsilon_1}))$  using the energy estimate (3.5) for any  $\delta \leq \varepsilon_1$ , so there exists a sequence  $(\mathbf{V}^{\delta_n^{(1)}}, P^{\delta_n^{(1)}})_{n \in \mathbb{N}}$  that weakly converges to  $(\mathbf{V}^{\varepsilon_1}, P^{\varepsilon_1}) \in L^2(\Gamma; (\mathbf{H}(\text{div}; \widehat{\Omega}_C^{\varepsilon_1}))^3 \times \mathbf{H}^1(\widehat{\Omega}_C^{\varepsilon_1}))$ . We consider the sequence of decreasing indices  $(\delta_n^{(1)})_{n \in \mathbb{N}}$  such that  $\delta_0^{(1)} \leq \varepsilon_2$ ,
2.  $(\mathbf{V}^{\delta_n^{(1)}}, P^{\delta_n^{(1)}})_{n \in \mathbb{N}}$  is bounded in  $L^2(\Gamma; (\mathbf{H}(\text{div}; \widehat{\Omega}_C^{\varepsilon_2})) \times \mathbf{H}^1(\widehat{\Omega}_C^{\varepsilon_2}))$  using the energy estimate (3.5) since  $\delta_n^{(1)} \leq \delta_0^{(1)} \leq \varepsilon_2$  for any  $n \in \mathbb{N}$ , so there exists a subsequence  $(\mathbf{V}^{\delta_n^{(2)}}, P^{\delta_n^{(2)}})_{n \in \mathbb{N}}$  that weakly converges to  $(\mathbf{V}^{\varepsilon_2}, P^{\varepsilon_2}) \in L^2(\Gamma; (\mathbf{H}(\text{div}; \widehat{\Omega}_C^{\varepsilon_2})) \times \mathbf{H}^1(\widehat{\Omega}_C^{\varepsilon_2}))$ . We consider the sequence of decreasing indices  $(\delta_n^{(2)})_{n \in \mathbb{N}}$  such that  $\delta_0^{(2)} \leq \varepsilon_3$ . Finally due to the extraction process, it holds that  $(\mathbf{V}^{\varepsilon_2}, P^{\varepsilon_2}) = (\mathbf{V}^{\varepsilon_1}, P^{\varepsilon_1})$  on  $\widehat{\Omega}_C^{\varepsilon_1}$ ,
3. iteratively for any  $k \geq 1$ ,  $(\mathbf{V}^{\delta_n^{(k)}}, P^{\delta_n^{(k)}})_{n \in \mathbb{N}}$  is bounded in  $L^2(\Gamma; (\mathbf{H}(\text{div}; \widehat{\Omega}_C^{\varepsilon_{k+1}})) \times \mathbf{H}^1(\widehat{\Omega}_C^{\varepsilon_{k+1}}))$  using the energy estimate (3.5) since  $\delta_n^{(k)} \leq \delta_0^{(k)} \leq \varepsilon_{k+1}$  for any  $n \in \mathbb{N}$ , so there exists a subsequence  $(\mathbf{V}^{\delta_n^{(k+1)}}, P^{\delta_n^{(k+1)}})_{n \in \mathbb{N}}$  that weakly converges to  $(\mathbf{V}^{\varepsilon_{k+1}}, P^{\varepsilon_{k+1}}) \in L^2(\Gamma; (\mathbf{H}(\text{div}; \widehat{\Omega}_C^{\varepsilon_{k+1}}))^3 \times \mathbf{H}^1(\widehat{\Omega}_C^{\varepsilon_{k+1}}))$ . We consider the sequence of decreasing indices  $(\delta_n^{(k+1)})_{n \in \mathbb{N}}$  such that  $\delta_0^{(k+1)} \leq \varepsilon_{k+2}$ . Finally due to the extraction process, it holds that  $(\mathbf{V}^{\varepsilon_{k+1}}, P^{\varepsilon_{k+1}}) = (\mathbf{V}^{\varepsilon_k}, P^{\varepsilon_k})$  on  $\widehat{\Omega}_C^{\varepsilon_k}$ .

We finally take the sequence  $(\mathbf{V}^{\delta^{(n)}}, P^{\delta^{(n)}})$ . By property of the intermediate sequence  $(\mathbf{V}_0^{\varepsilon_n}, P_0^{\varepsilon_n}), (\mathbf{V}^{\delta_n^{(n)}}, P^{\delta_n^{(n)}})$  weakly converges to  $(V_0, P_0)$  in  $L^2(\Gamma; \mathbf{H}(\text{div}, K)) \times L^2(\Gamma; \mathbf{H}^1(K))$  for any  $K \subset \widehat{\Omega}_C$  whose minimal to the boundary  $\{x_3 = 0\}$  is positive. Using (3.8), we obtain the following

**Proposition 3.2.** *There exists a scalar function  $V_0 \in L^2(\Gamma)$  such that*

$$\begin{aligned} \mathbf{V}_0(\mathbf{x}_\Gamma, x_3) &= V_0(\mathbf{x}_\Gamma) \sin\left(\frac{\omega}{c}(x_3 + L)\right) \mathbf{e}_3, \\ P_0(\mathbf{x}_\Gamma, x_3) &= -i\rho_0 c V_0(\mathbf{x}_\Gamma) \cos\left(\frac{\omega}{c}(x_3 + L)\right). \end{aligned} \quad (3.9)$$

**Conclusion:** Using the weak convergence of  $(\mathbf{V}^\delta, P^\delta)$  to  $(\mathbf{V}_0, P_0)$  and (3.9), we get the following limit interface conditions:

$$\begin{aligned} \lim_{\delta \rightarrow 0} \int_{\mathcal{A}_C} P^\delta(\mathbf{x}_\Gamma, -2\sqrt{\delta}, (y_1, y_2)) \, dy_1 \, dy_2 &= -a_C i \rho_0 c V_0(\mathbf{x}_\Gamma) \cos\left(\frac{\omega L}{c}\right), \\ \lim_{\delta \rightarrow 0} \int_{\mathcal{A}_C} \mathbf{V}^\delta(\mathbf{x}_\Gamma, -2\sqrt{\delta}, (y_1, y_2)) \cdot \mathbf{e}_3 \, dy_1 \, dy_2 &= a_C V_0(\mathbf{x}_\Gamma) \sin\left(\frac{\omega L}{c}\right). \end{aligned} \quad (3.10)$$

### 3.2 Weak convergence in the pattern below aperture

Again we consider for each  $\delta > 0$  and any  $\mathbf{x} \in \Omega^\delta \setminus \Omega$  the unique corresponding resonator position  $\mathbf{x}_\Gamma^\delta$  with  $\mathbf{x} \in \Omega_H^\delta(\mathbf{x}_\Gamma^\delta)$ . Then we define the zone below aperture as

$$\Omega_-^\delta(\mathbf{x}_\Gamma^\delta) := \left\{ \mathbf{x} \in \mathbf{x}_\Gamma^\delta + \delta \mathcal{A}_C \times (-2\sqrt{\delta}, -h_0 \delta^2) \text{ such that } \mathbf{x} \notin B_3(\mathbf{x}_\Gamma^\delta - \delta h_0 \mathbf{e}_3, \delta^{\frac{3}{2}}) \right\},$$

and the rescaled zone below aperture (see Fig. 4) for the variable change  $\mathbf{y} = \delta^{-1}(\mathbf{x} - \mathbf{x}_\Gamma^\delta)$

$$\mathcal{B}_-^\delta := \left\{ \mathbf{y} \in \mathcal{A}_C \times (-2/\sqrt{\delta}, -h_0 \delta) \text{ such that } \mathbf{y} \notin B_3(-\delta h_0 \mathbf{e}_3, \sqrt{\delta}) \right\},$$

where  $B_d(\mathbf{x}_0, r)$  denotes the  $d$ -dimensional ball centered at  $\mathbf{x}_0$  and of radius  $r$ .

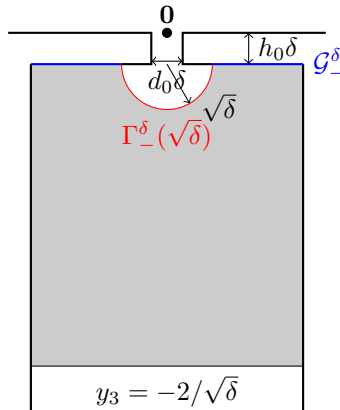


Figure 4: Illustration of the canonical domain  $\mathcal{B}_-^\delta$  for the pattern below aperture (gray).

Here, we are interested in the behaviour of the solution  $(\mathbf{v}^\delta, p^\delta)$  solution of (2.5) in the resonator array, close to the apertures. To do so, we introduce the five-dimensional functions  $\Psi_-^\delta$  and  $\Phi_-^\delta$  by

$$\Psi_-^\delta(\mathbf{x}_\Gamma^\delta, \mathbf{y}) = \mathbf{v}^\delta(\mathbf{x}_\Gamma^\delta + \delta\mathbf{y}) \quad \text{and} \quad \Phi_-^\delta(\mathbf{x}_\Gamma^\delta, \mathbf{y}) = p^\delta(\mathbf{x}_\Gamma^\delta + \delta\mathbf{y}). \quad (3.11)$$

Then, in view of estimate (3.1) of Lemma 3.1, the rescaled functions  $(\Psi_-^\delta, \Phi_-^\delta)$  satisfy the following estimate for almost all resonators

$$\begin{aligned} \delta \|\Psi_-^\delta(\mathbf{x}_\Gamma^\delta, \cdot)\|_{L^2(\mathcal{B}_-^\delta)}^2 + \frac{1}{\delta} \|\operatorname{div}_{\mathbf{y}} \Psi_-^\delta(\mathbf{x}_\Gamma^\delta, \cdot)\|_{L^2(\mathcal{B}_-^\delta)}^2 + \delta^3 \|\operatorname{curl}_{\mathbf{y}} \Psi_-^\delta(\mathbf{x}_\Gamma^\delta, \cdot)\|_{L^2(\mathcal{B}_-^\delta)}^2 \\ + \delta \|\Phi_-^\delta(\mathbf{x}_\Gamma^\delta, \cdot)\|_{L^2(\mathcal{B}_-^\delta)}^2 + \frac{1}{\delta} \|\nabla_{\mathbf{y}} \Phi_-^\delta(\mathbf{x}_\Gamma^\delta, \cdot)\|_{L^2(\mathcal{B}_-^\delta)}^2 \leq C_H \end{aligned} \quad (3.12)$$

We extend again this *discrete* error estimate into a *continuous* error estimate on  $L^2(\Gamma; L^2(\mathcal{B}_-^\delta))$ . This error estimate allows us to give some results about the rescaled functions.

**For the rescaled pressure  $\Phi_-^\delta$ ,** using the Cauchy-Schwartz inequality and the error estimate (3.12) leads to

$$\left( \int_{\mathcal{B}_-^\delta} |\nabla_{\mathbf{y}} \Phi_-^\delta(\mathbf{x}_\Gamma, \mathbf{y})| \, d\mathbf{y} \right)^2 \leq \frac{2}{\sqrt{\delta}} \int_{\mathcal{B}_-^\delta} |\nabla_{\mathbf{y}} \Phi_-^\delta(\mathbf{x}_\Gamma, \mathbf{y})|^2 \, d\mathbf{y} \leq 2C_H \sqrt{\delta}$$

and this quantity tends to 0 as  $\delta \rightarrow 0$ , so that the gradient of  $\Phi_-^\delta(\mathbf{x}_\Gamma, \cdot)$  tends to 0 almost everywhere in  $(-\infty, 0) \times \mathcal{A}_C$ . It remains to check that the average of  $\Phi_-^\delta$  remains uniformly bounded as well. This can be checked using again the energy estimate (3.12) and using that

$$\delta \|1\|_{L^2(\mathcal{B}_-^\delta)}^2 = \delta \left( a_C \left( \frac{2}{\sqrt{\delta}} - h_0 \delta \right) - \frac{2\pi}{3} \delta^{\frac{3}{2}} \right)^2.$$

We can then extract a subsequence (that we still denote by  $\Phi_-^\delta$ ) that converges to a constant. Using

$$P^\delta(\mathbf{x}_\Gamma, -\frac{2}{\sqrt{\delta}}, (y_1, y_2)) = p^\delta(\mathbf{x}_\Gamma + \delta(y_1, y_2, -\frac{2}{\sqrt{\delta}})) = \Phi_-^\delta(\mathbf{x}_\Gamma, (y_1, y_2, -\frac{2}{\sqrt{\delta}}))$$

for almost every  $(y_1, y_2) \in \mathcal{A}_C$  and the first line of (3.10), we obtain that

$$\lim_{\delta \rightarrow 0} \Phi_-^\delta = -i\rho_0 c V_0(\mathbf{x}_\Gamma) \cos\left(\frac{\omega L}{c}\right). \quad (3.13)$$

**Similarly, for the rescaled velocity  $\Psi_-^\delta$ ,** using the Cauchy-Schwartz inequality and the error estimate (3.12) leads to

$$\left( \int_{\mathcal{B}_-^\delta} |\operatorname{div}_{\mathbf{y}} \Psi_-^\delta(\mathbf{x}_\Gamma, \mathbf{y})| \, d\mathbf{y} \right)^2 \leq \frac{2}{\sqrt{\delta}} \int_{\mathcal{B}_-^\delta} |\operatorname{div}_{\mathbf{y}} \Psi_-^\delta(\mathbf{x}_\Gamma, \mathbf{y})|^2 \, d\mathbf{y} \leq 2C_H \sqrt{\delta},$$

and this quantity tends to 0 as  $\delta$  tends to 0. Using the Gauss theorem on  $\mathcal{B}_-^\delta$  gives

$$\begin{aligned} \int_{\mathcal{B}_-^\delta} \operatorname{div}_{\mathbf{y}} \Psi_-^\delta = \int_{\mathcal{A}_C} \Psi_-^\delta(\mathbf{x}_\Gamma, (y_1, y_2, -\frac{2}{\sqrt{\delta}})) \cdot (-\mathbf{e}_3) \, dy_1 \, dy_2 \\ + \int_{\Gamma_-^\delta(\sqrt{\delta})} \Psi_-^\delta(\mathbf{x}_\Gamma, \mathbf{y}) \cdot \mathbf{n}_-^\delta(\mathbf{y}) \, d\sigma(\mathbf{y}), \end{aligned}$$

where  $\mathbf{n}_-^\delta(\mathbf{y})$  is the unit outward vector of  $\mathcal{B}_-^\delta$ , *i. e.*,

$$\mathbf{n}_-^\delta(\mathbf{y}) = \frac{(y_1, y_2, -(y_3 + \delta h_0))}{|(y_1, y_2, -(y_3 + \delta h_0))|}.$$

Using then

$$\mathbf{V}^\delta(\mathbf{x}_\Gamma, -2\sqrt{\delta}, (y_1, y_2)) = \mathbf{v}^\delta(\mathbf{x}_\Gamma + \delta(y_1, y_2, -\frac{2}{\sqrt{\delta}})) = \mathbf{\Psi}_-^\delta(\mathbf{x}_\Gamma, (y_1, y_2, -\frac{2}{\sqrt{\delta}}))$$

and using the second line of relation (3.10) gives

$$\lim_{\delta \rightarrow 0} \int_{\Gamma_-^\delta(\sqrt{\delta})} \mathbf{\Psi}_-^\delta(\mathbf{x}_\Gamma, \mathbf{y}) \cdot \mathbf{n}_-^\delta(\mathbf{y}) d\sigma(\mathbf{y}) = a_C V_0(\mathbf{x}_\Gamma) \sin\left(\frac{\omega L}{c}\right). \quad (3.14)$$

### 3.3 Weak convergence in the apertures

For each  $\delta > 0$ , we consider  $\mathbf{x} \in \Omega^\delta$  and corresponding resonator position  $\mathbf{x}_\Gamma^\delta \in \Gamma^\delta$  such that one of the three following conditions is satisfied:

1.  $\mathbf{x}$  belongs to the neck  $\Omega_N^\delta(\mathbf{x}_\Gamma^\delta)$ ,
2.  $\mathbf{x}$  is inside the resonator chamber  $\Omega_C^\delta(\mathbf{x}_\Gamma^\delta)$ , and  $|\mathbf{x} - (\mathbf{x}_\Gamma^\delta, -\delta^2 h_0)| < 2\delta^{\frac{3}{2}}$ ,
3.  $\mathbf{x}$  is inside the domain  $\Omega$ , and  $|\mathbf{x} - (\mathbf{x}_\Gamma^\delta, 0)| < 2\delta^{\frac{3}{2}}$ ,

*i. e.*, the distance from  $\mathbf{x}$  to the neck  $\Omega_N^\delta(\mathbf{x}_\Gamma^\delta)$ , above and below the aperture, is at most  $2\delta^{\frac{3}{2}}$ . We introduce then the domain  $\Omega_A^\delta(\mathbf{x}_\Gamma^\delta)$  as the union of the neck  $\Omega_N^\delta(\mathbf{x}_\Gamma^\delta)$  and the two half-spheres of diameter  $2\delta^{\frac{3}{2}}$ , see Fig. 2(a), and we introduce the variable change  $\mathbf{x} = \mathbf{x}_\Gamma^\delta + \delta^2 \mathbf{z}$ , *i. e.*, it is equivalent to introduce the variable change  $\mathbf{y} = \delta \mathbf{z}$  in Section 3.2. As  $\mathbf{x}$  describes  $\Omega_A^\delta(\mathbf{x}_\Gamma^\delta)$ ,  $\mathbf{z}$  describes the domain  $\widehat{\Omega}(2\delta^{-1/2})$  that tends to the unbounded domain  $\widehat{\Omega}$  as  $\delta$  tends to 0, see Fig. 2(b) and Fig. 2(c). We also introduce the five-dimensional functions  $\mathbf{v}^\delta$  and  $\mathbf{p}^\delta$  by

$$\mathbf{v}^\delta(\mathbf{x}_\Gamma^\delta, \mathbf{z}) = \delta^2 \mathbf{v}^\delta(\mathbf{x}_\Gamma^\delta + \delta^2 \mathbf{z}) \quad \text{and} \quad \mathbf{p}^\delta(\mathbf{x}_\Gamma^\delta, \mathbf{z}) = p^\delta(\mathbf{x}_\Gamma^\delta + \delta^2 \mathbf{z}). \quad (3.15)$$

The scale change for the velocity  $\mathbf{v}^\delta$  is due to the following: for  $\mathbf{y} \in \Gamma_-^\delta(\sqrt{\delta})$ , *i. e.*, for  $\mathbf{z} \in \widehat{\Gamma}_-(1/\sqrt{\delta})$ , using the variable change  $\mathbf{y} = \delta \mathbf{z}$  leads to

$$\int_{\Gamma_-^\delta(\sqrt{\delta})} \mathbf{v}^\delta(\mathbf{x}_\Gamma^\delta + \delta \mathbf{y}) \cdot \mathbf{n}_-^\delta(\mathbf{y}) d\sigma(\mathbf{y}) = \delta^2 \int_{\widehat{\Gamma}_-(1/\sqrt{\delta})} \mathbf{v}^\delta(\mathbf{x}_\Gamma^\delta + \delta \mathbf{z}) \cdot \mathbf{n}_-^\delta(\delta \mathbf{z}) d\sigma(\mathbf{z}),$$

that leads to

$$\int_{\Gamma_-^\delta(\sqrt{\delta})} \mathbf{\Psi}_-^\delta(\mathbf{x}_\Gamma^\delta, \mathbf{y}) \cdot \mathbf{n}_-^\delta(\mathbf{y}) d\sigma(\mathbf{y}) = \int_{\widehat{\Gamma}_-(1/\sqrt{\delta})} \mathbf{v}^\delta(\mathbf{x}_\Gamma^\delta, \mathbf{z}) \cdot \mathbf{n}_-(\mathbf{z}) d\sigma(\mathbf{z}), \quad (3.16)$$

with

$$\mathbf{n}_-(\mathbf{z}) = \frac{(z_1, z_2, -(z_3 + h_0))}{|(z_1, z_2, -(z_3 + h_0))|}.$$



We consider the linearized Navier-Stokes problem (2.5) and we apply the isotropic coordinate change. Similarly to the derivation of problem (3.3), we obtain the following system

$$-i\omega \mathbf{v}^\delta + \frac{1}{\rho_0} \nabla_{\mathbf{z}} \mathbf{p}^\delta - \nu_0 \Delta_{\mathbf{z}} \mathbf{v}^\delta - \nu_0' \nabla_{\mathbf{z}} \operatorname{div}_{\mathbf{z}} \mathbf{v}^\delta = \mathbf{0}, \quad \text{in } \Gamma^\delta \times \widehat{\Omega}(2\delta^{-1/2}), \quad (3.17a)$$

$$-i\omega \delta^4 \mathbf{p}^\delta + \rho_0 c^2 \operatorname{div}_{\mathbf{z}} \mathbf{v}^\delta = 0, \quad \text{in } \Gamma^\delta \times \widehat{\Omega}(2\delta^{-1/2}), \quad (3.17b)$$

$$\mathbf{v}^\delta = \mathbf{0}, \quad \text{on } \Gamma^\delta \times \widehat{\Gamma}_A^\delta, \quad (3.17c)$$

where  $\widehat{\Gamma}_A^\delta := \partial \widehat{\Omega}(2\delta^{-1/2}) \cap \frac{1}{\delta^2} (\partial \Omega^\delta - \mathbf{x}_\Gamma^\delta)$  corresponds to the rescaled part of the boundary of  $\Omega^\delta$  in the vicinity of the neck centered at  $\mathbf{x}_\Gamma^\delta$  (depicted in blue on Fig. 2(b)), and tends to  $\partial \widehat{\Omega}$  as  $\delta$  tends to 0.

Again, in view of estimate (3.1) of Lemma 3.1, the rescaled functions  $(\mathbf{v}^\delta, \mathbf{p}^\delta)$  satisfy the following estimate for almost all resonators

$$\begin{aligned} & \|\mathbf{v}^\delta(\mathbf{x}_\Gamma^\delta, \cdot)\|_{L^2(\widehat{\Omega}(2\delta^{-1/2}))}^2 + \frac{1}{\delta^4} \|\operatorname{div}_{\mathbf{z}} \mathbf{v}^\delta(\mathbf{x}_\Gamma^\delta, \cdot)\|_{L^2(\widehat{\Omega}(2\delta^{-1/2}))}^2 + \|\mathbf{curl}_{\mathbf{z}} \mathbf{v}^\delta(\mathbf{x}_\Gamma^\delta, \cdot)\|_{L^2(\widehat{\Omega}(2\delta^{-1/2}))}^2 \\ & + \delta^4 \|\mathbf{p}^\delta(\mathbf{x}_\Gamma^\delta, \cdot)\|_{L^2(\widehat{\Omega}(2\delta^{-1/2}))}^2 + \|\nabla \mathbf{p}^\delta(\mathbf{x}_\Gamma^\delta, \cdot)\|_{L^2(\widehat{\Omega}(2\delta^{-1/2}))}^2 \leq C_H \end{aligned} \quad (3.18)$$

We extend then the discrete problem (3.17) into a continuous problem on the resonator position  $\mathbf{x}_\Gamma \in \Gamma$  and the error estimate (3.18) into an  $L^2(\Gamma; L^2(\widehat{\Omega}(2\delta^{-1/2})))$  estimate. The sequence  $\mathbf{v}^\delta$  is bounded in  $L^2(\Gamma; \mathbf{H}(\operatorname{div}, D) \cap \mathbf{H}(\mathbf{curl}, D))$  for any bounded open set  $D$  included in  $\widehat{\Omega}$  and for any  $\delta$  such that  $D \subset \widehat{\Omega}(2\delta^{-1/2})$ , then we can extract a subsequence (still denoted by  $\mathbf{v}^\delta$ ) that converges weakly in  $L^2(\Gamma; \mathbf{H}(\operatorname{div}, D) \cap \mathbf{H}(\mathbf{curl}, D))$ . Taking iteratively  $D = D^n := \widehat{\Omega}_A \cap \mathcal{B}(\mathbf{0}, 2^n)$ , we state that  $\mathbf{v}^\delta$  admits a subsequence that converges weakly to a function  $\mathbf{v}_{-2}$  in  $L^2(\Gamma; \mathbf{H}(\operatorname{div}, \widehat{\Omega}) \cap \mathbf{H}(\mathbf{curl}, \widehat{\Omega}))$ , the subscript “-2” relates to the shift in  $\delta$  for the function  $\mathbf{v}^\delta$ . We deduce moreover from the first line of (3.18) and using the lower semi-continuity that  $\operatorname{div} \mathbf{v}_{-2} = 0$  in  $\widehat{\Omega}$ . Similarly, the sequence  $\mathbf{p}^\delta$  is bounded in  $L^2(\Gamma; \mathcal{V}(D))$  for any bounded open set  $D$  included in  $\widehat{\Omega}$  and for any  $\delta$  such that  $D \subset \widehat{\Omega}(2\delta^{-1/2})$ , where

$$\mathcal{V}(D) = \left\{ \mathbf{p} \in L^2_{\text{loc}}(D) \text{ such that } \nabla \mathbf{p} \in L^2(D)^3 \right\},$$

then doing a similar construction, this sequence admits a subsequence that converges weakly to  $\nabla_{\mathbf{z}} \mathbf{p}_0$  in  $\mathcal{V}(\widehat{\Omega})$ . Using then the weak convergence in the continuity equation (3.17a), we get that the weak limit  $(\mathbf{v}_{-2}, \mathbf{p}_0)$  is solution of the following instationary Stokes problem

$$-i\omega \mathbf{v}_{-2}(\mathbf{x}_\Gamma, \cdot) + \frac{1}{\rho_0} \nabla_{\mathbf{z}} \mathbf{p}_0(\mathbf{x}_\Gamma, \cdot) - \nu_0 \Delta_{\mathbf{z}} \mathbf{v}_{-2}(\mathbf{x}_\Gamma, \cdot) = \mathbf{0}, \quad \text{in } \widehat{\Omega}, \quad (3.19a)$$

$$\operatorname{div}_{\mathbf{z}} \mathbf{v}_{-2}(\mathbf{x}_\Gamma, \cdot) = 0, \quad \text{in } \widehat{\Omega}, \quad (3.19b)$$

$$\mathbf{v}_{-2}(\mathbf{x}_\Gamma, \cdot) = \mathbf{0}, \quad \text{on } \partial \widehat{\Omega}. \quad (3.19c)$$

Note that this problem can be written equivalently with a  $\mathbf{curl}_{\mathbf{z}} \mathbf{curl}_{\mathbf{z}}$  operator instead of the  $-\Delta_{\mathbf{z}}$  operator, since  $\operatorname{div}_{\mathbf{z}} \mathbf{v}_{-2}(\mathbf{x}_\Gamma, \cdot) = 0$ . Taking the divergence gives that  $p_0(\mathbf{x}_\Gamma, \cdot)$  is an harmonic function on  $\widehat{\Omega}$ , so that its behaviour towards infinity is described using spherical functions[20]. Then, following an expansion of  $\mathbf{v}_{-2}$  as a sum of spherical functions and functions that are exponentially decaying with respect to the distance to the boundary  $\partial \widehat{\Omega}$ , the only spherical harmonics on a half-sphere that lead

to  $\mathbf{v}_{-2}(\mathbf{x}_\Gamma, \cdot) \in \mathbf{H}(\operatorname{div}, \widehat{\Omega}) \cap \mathbf{H}(\operatorname{curl}, \widehat{\Omega})$  are the spherical harmonics that admit a behaviour at most constant towards infinity, the constants at both sides of the wall can be different. Therefore, we seek for two functions  $c_m$  and  $c_j$  defined on  $\Gamma$  such that

$$(\mathbf{v}_{-2}(\mathbf{x}_\Gamma, \mathbf{z}), \mathbf{p}_0(\mathbf{x}_\Gamma, \mathbf{z})) = c_m(\mathbf{x}_\Gamma)(\mathbf{0}, 1) + c_j(\mathbf{x}_\Gamma)(\mathbf{v}(\mathbf{z}), \mathbf{p}(\mathbf{z})), \quad (3.20)$$

where the *neck profile*  $(\mathbf{v}, \mathbf{p}) \in (\mathbf{H}(\operatorname{div}, \widehat{\Omega}) \cap \mathbf{H}(\operatorname{curl}, \widehat{\Omega})) \times \mathcal{V}(\widehat{\Omega})$  is solution of the instationary Stokes problem

$$-i\omega \mathbf{v} + \frac{1}{\rho_0} \nabla_{\mathbf{z}} \mathbf{p} - \nu_0 \Delta_{\mathbf{z}} \mathbf{v} = \mathbf{0}, \quad \text{in } \widehat{\Omega}, \quad (3.21a)$$

$$\operatorname{div}_{\mathbf{z}} \mathbf{v} = 0, \quad \text{in } \widehat{\Omega}, \quad (3.21b)$$

$$\mathbf{v} = \mathbf{0}, \quad \text{on } \partial \widehat{\Omega}, \quad (3.21c)$$

completed by Dirichlet jump conditions at infinity

$$\lim_{S \rightarrow \infty} \mathbf{p}|_{\widehat{\Gamma}_{\pm}(S)} = \pm \frac{1}{2}, \quad (3.21d)$$

where the half-spheres  $\widehat{\Gamma}_{\pm}(S)$  for  $S > 0.5d_0$  are given by

$$\begin{aligned} \widehat{\Gamma}_{\pm}(S) = \{ \mathbf{z} \in \widehat{\Omega} \text{ such that } |\mathbf{z} - (\pm 0.5 - 0.5)h_0 \mathbf{e}_3| = S \\ \text{and } \pm (\mathbf{z} \cdot \mathbf{e}_3 \mp 0.5h_0 + 0.5h_0) > 0 \}. \end{aligned} \quad (3.22)$$

and are depicted on Fig. 2(c).

Let us take  $S > 0.5d_0$ . We denote by  $\widehat{\Omega}(S)$  the subdomain of  $\widehat{\Omega}$  that is delimited by  $\widehat{\Gamma}_-(S)$  and  $\widehat{\Gamma}_+(S)$ . Since the function  $\mathbf{v}$  is divergence-free in  $\widehat{\Omega}(S)$  and its trace vanishes on  $\partial \widehat{\Omega}$ , it turns out immediately that

$$\int_{\widehat{\Gamma}_+(S)} \tilde{\mathbf{v}} \cdot \mathbf{n} + \int_{\widehat{\Gamma}_-(S)} \tilde{\mathbf{v}} \cdot \mathbf{n} = 0,$$

where  $\mathbf{n}$  is the unit outward normal vector. Following the formulation of the Rayleigh conductivity  $K_R$ [38, 39] which describes the ratio of the fluctuating volume flow to the driving pressure difference, we introduce the *effective Rayleigh conductivity*  $k_R$  as

$$k_R := \lim_{S \rightarrow \infty} \frac{i\omega \rho_0}{2} \left( \int_{\widehat{\Gamma}_+(S)} \tilde{\mathbf{v}} \cdot \mathbf{n} - \int_{\widehat{\Gamma}_-(S)} \tilde{\mathbf{v}} \cdot \mathbf{n} \right). \quad (3.23)$$

Existence and uniqueness of problem (3.21) is stated by Proposition 2.1, and properties of the effective Rayleigh coefficient  $k_R$  is stated by Proposition 2.2.

It remains to determine the conditions at infinity satisfied by  $(\mathbf{v}, \mathbf{p})$ , using that for almost any  $\mathbf{y} \in \Gamma_{-}^{\delta}(\sqrt{\delta})$ ,

$$\Psi_{-}^{\delta}(\mathbf{x}_\Gamma, \mathbf{y}) = \mathbf{v}^{\delta}(\mathbf{x}_\Gamma + \delta \mathbf{y}) = \mathbf{v}^{\delta}\left(\mathbf{x}_\Gamma, \frac{\mathbf{y}}{\delta}\right),$$

$$\Phi_{-}^{\delta}(\mathbf{x}_\Gamma, \mathbf{y}) = p^{\delta}(\mathbf{x}_\Gamma + \delta \mathbf{y}) = p^{\delta}\left(\mathbf{x}_\Gamma, \frac{\mathbf{y}}{\delta}\right).$$

**For the rescaled velocity  $\mathbf{v}^{\delta}$** , we use relations (3.14), (3.16) and (3.20), coupled with the definition of the effective Rayleigh conductivity  $k_R$ , to obtain

$$a_C V_0(\mathbf{x}_\Gamma) \sin\left(\frac{\omega L}{c}\right) = \frac{k_R}{i\rho_0 \omega} c_j(\mathbf{x}_\Gamma).$$

Using the solution representation (3.20), we obtain the following relation

$$\lim_{\delta \rightarrow 0} \int_{\widehat{\Gamma}_+(1/\sqrt{\delta})} \mathbf{v}^\delta(\mathbf{x}_\Gamma, \mathbf{z}) \cdot \mathbf{n}_+(\mathbf{z}) \, d\sigma(\mathbf{z}) = c_j(\mathbf{x}_\Gamma) = \frac{i\rho_0\omega a_C}{k_R} V_0(\mathbf{x}_\Gamma) \sin\left(\frac{\omega L}{c}\right), \quad (3.24)$$

where

$$\mathbf{n}_+(\mathbf{z}) = \frac{(-z_1 - z_2, z_3)}{|(-z_1, -z_2, z_3)|}.$$

**For the rescaled pressure  $p^\delta$ ,** we use relations (3.13) and (3.20) to obtain

$$-i\rho_0 c V_0(\mathbf{x}_\Gamma) \cos\left(\frac{\omega L}{c}\right) = c_m(\mathbf{x}_\Gamma) - 0.5c_j(\mathbf{x}_\Gamma).$$

Using the again the solution representation (3.20), we obtain the following relation

$$\lim_{\delta \rightarrow 0} p^\delta(\mathbf{x}_\Gamma, \cdot)|_{\widehat{\Gamma}_+(1/\sqrt{\delta})} = -i\rho_0 c V_0(\mathbf{x}_\Gamma) \cos\left(\frac{\omega L}{c}\right) + \frac{i\rho_0\omega a_C}{k_R} V_0(\mathbf{x}_\Gamma) \sin\left(\frac{\omega L}{c}\right). \quad (3.25)$$

### 3.4 Weak convergence in the pattern above aperture

Similarly to the formal derivation in the pattern below aperture in Section 3.2, for each  $\delta > 0$  we consider  $\mathbf{x} \in \Omega$  and corresponding resonator position  $\mathbf{x}_\Gamma^\delta$  such that  $\mathbf{x} \in \Omega_H^\delta(\mathbf{x}_\Gamma^\delta)$ . Then we define the zone above aperture

$$\Omega_+^\delta(\mathbf{x}_\Gamma^\delta) := \left\{ \mathbf{x} \in \mathbf{x}_\Gamma^\delta + \delta\mathcal{A} \times (0, 2\sqrt{\delta}) \text{ such that } \mathbf{x} \notin B_3(\mathbf{x}_\Gamma^\delta, \delta^{\frac{3}{2}}) \right\},$$

and the rescaled zone below aperture (see Fig. 5) for the variable change  $\mathbf{y} = \delta^{-1}(\mathbf{x} - \mathbf{x}_\Gamma^\delta)$ .

Here, we are interested in the behaviour of the solution  $\mathbf{v}^\delta, p^\delta$  solution of (2.5) in the domain  $\Omega$ , close to the apertures. To do so, we introduce the five-dimensional functions  $\Psi_+^\delta$  and  $\Phi_+^\delta$  by

$$\Psi_+^\delta(\mathbf{x}_\Gamma^\delta, \mathbf{y}) = \mathbf{v}^\delta(\mathbf{x}_\Gamma^\delta + \delta\mathbf{y}) \quad \text{and} \quad \Phi_+^\delta(\mathbf{x}_\Gamma^\delta, \mathbf{y}) = \frac{1}{\delta} p^\delta(\mathbf{x}_\Gamma^\delta + \delta\mathbf{y}), \quad (3.26)$$

similarly to the introduction of the functions  $\Psi_-^\delta$  and  $\Phi_-^\delta$  in (3.11).

Then, in view of estimate (3.1) of Lemma 3.1 the rescaled functions  $(\Psi_-^\delta, \Phi_-^\delta)$  satisfy the following estimate for almost all resonator

$$\begin{aligned} \delta \|\Psi_+^\delta(\mathbf{x}_\Gamma^\delta, \cdot)\|_{L^2(\mathcal{B}_+^\delta)}^2 + \frac{1}{\delta} \|\operatorname{div}_{\mathbf{y}} \Psi_+^\delta(\mathbf{x}_\Gamma^\delta, \cdot)\|_{L^2(\mathcal{B}_+^\delta)}^2 + \delta^3 \|\operatorname{curl}_{\mathbf{y}} \Psi_+^\delta(\mathbf{x}_\Gamma^\delta, \cdot)\|_{L^2(\mathcal{B}_+^\delta)}^2 \\ + \delta \|\Phi_+^\delta(\mathbf{x}_\Gamma^\delta, \cdot)\|_{L^2(\mathcal{B}_+^\delta)}^2 + \frac{1}{\delta} \|\nabla_{\mathbf{y}} \Phi_+^\delta(\mathbf{x}_\Gamma^\delta, \cdot)\|_{L^2(\mathcal{B}_+^\delta)}^2 \leq C_H. \end{aligned} \quad (3.27)$$

We extend again this *discrete* error estimate into a *continuous* error estimate on  $L^2(\Gamma, L^2(\mathcal{B}_+^\delta))$ .

This error estimate allows us to give some results about the rescaled functions.

**For the rescaled pressure  $\Phi_+^\delta$ ,** using the Cauchy-Schwartz inequality and the error estimate (3.27) leads to

$$\left( \int_{\mathcal{B}_+^\delta} |\nabla_{\mathbf{y}} \Phi_+^\delta(\mathbf{x}_\Gamma, \mathbf{y})| \, d\mathbf{y} \right)^2 \leq \frac{2}{\sqrt{\delta}} \int_{\mathcal{B}_+^\delta} |\nabla_{\mathbf{y}} \Phi_+^\delta(\mathbf{x}_\Gamma, \mathbf{y})|^2 \, d\mathbf{y} \leq 2C_H \sqrt{\delta},$$

and this quantity tends to 0 as  $\delta \rightarrow 0$ , so that the gradient of  $\Phi_+^\delta(\mathbf{x}_\Gamma, \cdot)$  tends to 0 almost everywhere in  $\mathcal{A} \times (0, \infty)$ . It remains to check that the average of  $\Phi_+^\delta$  remains

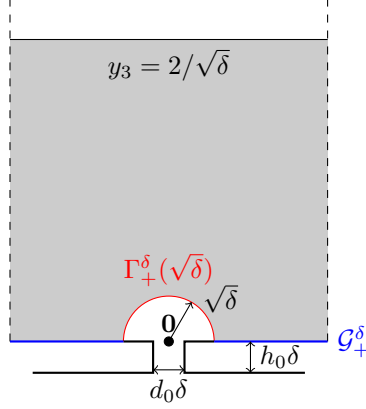


Figure 5: Representation of the canonical domain  $\mathcal{B}_+^\delta$  for the pattern above aperture (gray).

uniformly bounded as well. This can be checked using again the energy estimate (3.27) and using that

$$\delta \|1\|_{L^2(\mathcal{B}_+^\delta)}^2 = \delta \left( \frac{2}{\sqrt{\delta}} - \frac{2\pi}{3} \delta^{\frac{3}{2}} \right)^2.$$

We can then extract a subsequence (that we still denote by  $\Phi_-^\delta$ ) that converges to a constant. Using

$$\mathbf{p}^\delta(\mathbf{x}_\Gamma, \delta^{-1}\mathbf{y}) = p^\delta(\mathbf{x}_\Gamma + \delta\mathbf{y}) = \Phi_-^\delta(\mathbf{x}_\Gamma, \mathbf{y})$$

for almost every  $\mathbf{y} \in \Sigma_+^\delta(\sqrt{\delta})$  and (3.25), we obtain that

$$\lim_{\delta \rightarrow 0} \Phi_+^\delta = -i\rho_0 c V_0(\mathbf{x}_\Gamma) \cos\left(\frac{\omega L}{c}\right) + \frac{i\rho_0 \omega a_C}{k_R} V_0(\mathbf{x}_\Gamma) \sin\left(\frac{\omega L}{c}\right). \quad (3.28)$$

**Similarly, for the rescaled velocity  $\Psi_+^\delta$ ,** using the Cauchy-Schwartz inequality leads to

$$\left( \int_{\mathcal{B}_+^\delta} |\operatorname{div}_{\mathbf{y}} \Psi_+^\delta(\mathbf{x}_\Gamma, \mathbf{y})| \, d\mathbf{y} \right)^2 \leq \frac{2}{\sqrt{\delta}} \int_{\mathcal{B}_+^\delta} |\operatorname{div}_{\mathbf{y}} \Psi_+^\delta(\mathbf{x}_\Gamma, \mathbf{y})|^2 \, d\mathbf{y} \leq 2C_H \sqrt{\delta},$$

and this quantity tends to 0 as  $\delta$  tends to 0. Using the Gauss theorem on  $\mathcal{B}_+^\delta$  gives

$$\begin{aligned} \int_{\mathcal{B}_+^\delta} \operatorname{div}_{\mathbf{y}} \Psi_+^\delta &= \int_{\mathcal{A}} \Psi_+^\delta(\mathbf{x}_\Gamma, (y_1, y_2, \frac{2}{\sqrt{\delta}})) \cdot \mathbf{e}_3 \, dy_1 \, dy_2 \\ &- \int_{\Gamma_+^\delta(\sqrt{\delta})} \Psi_+^\delta(\mathbf{x}_\Gamma, \mathbf{y}) \cdot \mathbf{n}_+(\mathbf{y}) \, d\sigma(\mathbf{y}) + \int_0^{2/\sqrt{\delta}} \int_{\partial\mathcal{A}_C} \Psi_+^\delta(\mathbf{x}_\Gamma, \mathbf{y}) \cdot \mathbf{n} \, d\sigma(y_1, y_2) \, dy_3. \end{aligned}$$

Since  $\mathcal{A}$  is a parallelogram driven by the two vectors  $(\mathbf{a}_i)_{i \in \{1,2\}}$ , we call  $\Gamma_{\mathcal{A},i}$  the edge of  $\mathcal{A}$  such that  $\Gamma_{\mathcal{A},i} + \mathbf{a}_i$  is also one edge of  $\mathcal{A}$ . Then, for  $\mathbf{x}_\Gamma \in \Gamma$  and  $\mathbf{y} \in \Gamma_{\mathcal{A},i} \times (0, \infty)$ , we consider the point  $\mathbf{x} := \mathbf{x}_\Gamma + \delta\mathbf{y} + \delta\mathbf{a}_i$  that corresponds locally to a common boundary of the two semi-infinite strips centered respectively at  $\mathbf{x}_\Gamma$  and  $\mathbf{x}_\Gamma + \delta\mathbf{a}_i$ :

$$\Psi_+^\delta(\mathbf{x}_\Gamma, \mathbf{y} + \mathbf{a}_i) = \mathbf{v}^\delta(\mathbf{x}_\Gamma + \delta\mathbf{y} + \delta\mathbf{a}_i) = \Psi_+^\delta(\mathbf{x}_\Gamma + \delta\mathbf{a}_i, \mathbf{y}). \quad (3.29)$$

Since both the norms of  $\operatorname{div} \Psi_+^\delta$  and  $\operatorname{curl} \Psi_+^\delta$  are decaying to 0 using (3.27), the norm of the gradient of each component of  $\Psi_+^\delta$  also tends to 0 as  $\delta$  tends to 0. Using

$$\Psi_+^\delta(\mathbf{x}_\Gamma, \mathbf{y} + \mathbf{a}_i) = \Psi_+^\delta(\mathbf{x}_\Gamma, \mathbf{y}) + \int_0^1 \nabla \Psi_+^\delta(\mathbf{x}_\Gamma, \mathbf{y} + t\mathbf{a}_i) \cdot \mathbf{a}_i dt,$$

we deduce that

$$\lim_{\delta \rightarrow 0} \int_0^{2/\sqrt{\delta}} \int_{\partial \mathcal{A}_C} \Psi_+(\mathbf{x}_\Gamma, \mathbf{y}) \cdot \mathbf{n} d\sigma(y_1, y_2) dy_3 = 0.$$

Using finally (3.24), we obtain

$$\lim_{\delta \rightarrow 0} \int_{\mathcal{A}} \Psi_+^\delta(\mathbf{x}_\Gamma, (y_1, y_2, \frac{2}{\sqrt{\delta}})) \cdot \mathbf{e}_3 dy_1 dy_2 = a_C V_0(\mathbf{x}_\Gamma) \sin\left(\frac{\omega L}{c}\right). \quad (3.30)$$

### 3.5 Weak convergence in the macroscopic region

Now, we are interested in the behaviour of the solution  $(\mathbf{v}^\delta, p^\delta)$  of (2.5). Using the assumption estimate (2.15), there exists a subsequence that weakly converges to a limit  $(\mathbf{v}_0, p_0)$  in  $\mathbb{H}(\operatorname{div}, \Omega) \times \mathbb{H}^1(\Omega)$ .

The weak convergence applied to the continuity equation (2.5b) gives immediately the second line of (2.11). Multiplying the momentum equation (2.5a) by a test function  $\mathbf{w} \in \mathbb{H}(\operatorname{div}; \Omega) \cap \mathbb{H}(\operatorname{curl}; \Omega)$  such that  $\mathbf{w} = 0$  on  $\partial\Omega$  and using the Gauss theorem leads to

$$\begin{aligned} -i\omega \langle \mathbf{v}^\delta, \mathbf{w} \rangle_\Omega + \frac{1}{\rho_0} \langle \nabla \rho^\delta, \mathbf{w} \rangle_\Omega + \nu_0 \delta^4 \langle \operatorname{curl} \mathbf{v}^\delta, \operatorname{curl} \mathbf{w} \rangle_\Omega \\ + (\nu_0 + \nu'_0) \delta^4 \langle \operatorname{div} \mathbf{v}^\delta, \operatorname{div} \mathbf{w} \rangle_\Omega = \langle \mathbf{f}, \mathbf{w} \rangle_\Omega. \end{aligned}$$

Using then the weak convergence associated to the boundness of the norms  $\delta^2 \|\operatorname{curl} \mathbf{v}^\delta\|_{L^2(\Omega)}$  and  $\|\operatorname{div} \mathbf{v}^\delta\|_{L^2(\Omega)}$  leads to the first line of (2.11).

Next point is to derive the boundary condition. The easiest part is to derive the boundary condition on  $\partial\Omega \setminus \Gamma$ . Indeed, the trace operator

$$\begin{aligned} \gamma_0 : \quad \mathbb{H}(\operatorname{div}; \Omega) &\rightarrow L^2(\partial\Omega \setminus \Gamma), \\ \mathbf{v} &\mapsto \mathbf{v} \cdot \mathbf{n}, \end{aligned}$$

is a lower semi-continuous operator, and since  $\mathbf{v}^\delta$  weakly converges to  $\mathbf{v}_0$  in  $\mathbb{H}(\operatorname{div}; \Omega)$ , one has

$$\|\mathbf{v}_0 \cdot \mathbf{n}\|_{L^2(\partial\Omega \setminus \Gamma)} \leq \liminf_{\delta \rightarrow 0} \|\mathbf{v}^\delta \cdot \mathbf{n}\|_{L^2(\partial\Omega \setminus \Gamma)} = 0.$$

Determination of the boundary condition on  $\Gamma$  is more involved, and need the matching with the solution in the pattern above apertures. Indeed, for a particular resonator position  $\mathbf{x}_\Gamma \in \Gamma$ , we consider the domain  $\mathcal{O}_+^\delta = \mathbf{x}_\Gamma^\delta + \delta \mathcal{A} \times (\sqrt{\delta}, 2\sqrt{\delta}) \subset \Omega$ . We can moreover see that the point  $\mathbf{y} := \delta^{-1}(\mathbf{x} - \mathbf{x}_\Gamma)$  belongs to  $\mathcal{B}_+^\delta$ . Then, similarly to the writing of the conditions (3.13) and (3.14), we get the matching

$$\begin{aligned} \int_{\mathcal{A}} p^\delta(\mathbf{x}_\Gamma + \delta(y_1, y_2, \frac{2}{\sqrt{\delta}})) d(y_1, y_2) &= \int_{\mathcal{A}} \Phi_+^\delta(\mathbf{x}_\Gamma, (y_1, y_2, \frac{2}{\sqrt{\delta}})) d(y_1, y_2), \\ \int_{\mathcal{A}} \mathbf{v}^\delta(\mathbf{x}_\Gamma + \delta(y_1, y_2, \frac{2}{\sqrt{\delta}})) \cdot \mathbf{e}_3 d(y_1, y_2) &= \int_{\mathcal{A}} \Psi_+^\delta(\mathbf{x}_\Gamma, (y_1, y_2, \frac{2}{\sqrt{\delta}})) \mathbf{e}_3 d(y_1, y_2). \end{aligned} \quad (3.31)$$

The right-hand sides of (3.31) are treated using (3.28) and (3.30), respectively. The left-hand sides are treated using the  $L^2$  weak convergence of  $\mathbf{v}^\delta \cdot \mathbf{e}_3$  and  $p^\delta$  to  $\mathbf{v}_0 \cdot \mathbf{e}_3$  and  $p_0$  respectively and using an elliptic regularity result. Therefore, it holds

$$\begin{aligned} \mathbf{v}_0(\mathbf{x}_\Gamma) \cdot \mathbf{e}_3 &= a_C \sin\left(\frac{\omega L}{c}\right) V_0(\mathbf{x}_\Gamma), \\ p_0(\mathbf{x}_\Gamma) &= \left(-i\omega\rho_0 \cos\left(\frac{\omega L}{c}\right) + \frac{i\omega a_C \rho_0}{k_R} \sin\left(\frac{\omega L}{c}\right)\right) V_0(\mathbf{x}_\Gamma), \end{aligned} \quad (3.32)$$

where the function  $V_0(\mathbf{x}_\Gamma)$  is still unknown. It can still be eliminated so that the first line of (2.11) is also proved as well.

### 3.6 Uniqueness of the limit

We recall here the statement of the Lemma 2.4 about the existence and uniqueness of the limit problem (2.11): let  $\mathbf{f} \in H(\operatorname{div}; \Omega)$ , then there exists a unique solution  $(\mathbf{v}_0, p_0) \in H(\operatorname{div}; \Omega) \times H^1(\Omega)$ , except for frequencies  $\omega \in \Lambda$ , where  $\Lambda$  is a subset of  $\frac{\pi c}{L}\mathbb{N}$ .

*Proof of Lemma 2.4.* Due to the equivalence of problems (2.11) and (2.12), and since  $\operatorname{div} \mathbf{f} \in L^2(\Omega)$ , we seek for a solution  $p_0 \in H^1(\Omega)$  of this problem. Multiplying the first line of (2.12) by a test function  $q \in H^1(\Omega)$  and integrating by parts, the variational formulation associated to this problem is: find  $p_0 \in H^1(\Omega)$  such that, for any  $q \in H^1(\Omega)$ ,

$$\langle p_0, q \rangle_{H^1(\Omega)} - \left(1 + \frac{\omega^2}{c^2}\right) \langle p_0, q \rangle_{L^2(\Omega)} + b_\Gamma(p_0, q) = -\rho_0 \langle \operatorname{div} \mathbf{f}, q \rangle_{L^2(\Omega)}, \quad (3.33)$$

where  $\langle p_0, q \rangle_{H^1(\Omega)}$  (respectively  $\langle p_0, q \rangle_{L^2(\Omega)}$ ) is the inner scalar product of  $p_0$  and  $q$  in  $H^1(\Omega)$  (resp. in  $L^2(\Omega)$ ), and  $b_\Gamma(p_0, q)$  is the boundary operator given by

$$b_\Gamma(p_0, q) := \frac{\sin\left(\frac{\omega L}{c}\right)}{\frac{c}{\omega a_C} \cos\left(\frac{\omega L}{c}\right) - \frac{2}{k_R} \sin\left(\frac{\omega L}{c}\right)} \langle p_0, q \rangle_{L^2(\Gamma)}. \quad (3.34)$$

Since  $\operatorname{Im}(k_R) > 0$  and all other quantities of the expression  $\frac{c}{\omega a_C} \cos\left(\frac{\omega L}{c}\right) - \frac{2}{k_R} \sin\left(\frac{\omega L}{c}\right)$  are real-valued, that expression never vanishes. The subspace  $H^1(\Omega)$  is compactly embedded in  $L^2(\Omega)$  by the Rellich-Kondrachev theorem, cf. Chapter 2 of the book of Braess[9]. Similarly, the trace operator  $\gamma_0 : u \mapsto u|_\Gamma$  is a continuous operator from  $H^1(\Omega)$  to  $H^{1/2}(\Gamma)$ , and again the subspace  $H^{1/2}(\Gamma)$  is compactly embedded into  $L^2(\Gamma)$ . Hence the left-hand side of the variational formulation (3.33) can be written under the form  $\langle (I + K)p_0, q \rangle_{H^1(\Omega)}$ , where the operator  $I$  is the identity operator and the operator  $K$  defined by

$$\langle Kp, q \rangle_{H^1(\Omega)} := -\left(1 + \frac{\omega^2}{c^2}\right) \langle p, q \rangle_{L^2(\Omega)} + b_\Gamma(p, q), \quad \forall p, q \in H^1(\Omega),$$

is compact. Hence, the sum  $I + K$  is a Fredholm operator of index 0[45], *i. e.*, the dimension of its kernel coincides with the co-dimension of its range, and by the Fredholm alternative uniqueness implies existence.

Assume now that  $\langle (I + K)p_0, q \rangle_{H^1(\Omega)} = 0$  for any test function  $q \in H^1(\Omega)$ . From now on, we consider two different cases, depending on the nature of the operator  $b_\Gamma$ :

1.  $\sin\left(\frac{\omega L}{c}\right) = 0$ , *i. e.*,  $\omega \in \frac{\pi c}{L}\mathbb{N}$ . In that case, the problem admits a unique solution when  $\frac{\omega^2}{c^2}$  is not an eigenvalue of the  $-\Delta$  operator in  $\Omega$ . We denote then by  $\Lambda$  the subset of  $\frac{\pi c}{L}\mathbb{N}$  such that  $\frac{\omega^2}{c^2}$  is also an eigenvalue of the  $-\Delta$  operator in  $\Omega$ .

2.  $\sin\left(\frac{\omega L}{c}\right) \neq 0$ , i. e.,  $\omega \notin \frac{\pi c}{L}\mathbb{N}$ . In that case, taking the particular test function  $q = \overline{p_0}$  and then the imaginary part of  $\langle (I + K)p_0, \overline{p_0} \rangle_{H^1(\Omega)}$ , we find that  $\text{Im } b_\Gamma(p_0, \overline{p_0}) = 0$ . Hence  $p_0$  vanishes on  $\Gamma$ . Due to the boundary condition on  $\Gamma$ , also  $\nabla p_0 \cdot \mathbf{n}$  vanishes on  $\Gamma$ . Using then the unique continuation theorem on elliptic operators[37] (see also Section 4.3 of the book of Leis[29]), we deduce that  $p_0$  vanishes in whole  $\Omega$  and therefore existence and uniqueness of a solution  $p_0$  of (2.12) follow.

□

Existence and uniqueness of Lemma 2.4 states that the whole sequence  $(\mathbf{v}_\delta, p_\delta)$  weakly converges to  $(\mathbf{v}_0, p_0)$  is  $H(\text{div}, \Omega) \times H^1(\Omega)$ , and not only a subsequence.

## 4 Numerical simulations

In this section we describe first how we compute numerically the effective Rayleigh conductivity  $k_R$  (Section 4.1), study the normalized specified acoustic impedance as a function of frequency (Section 4.2) and the frequency-dependent dissipation in a waveguide predicted by the derived model (Section 4.3) in comparison with existing models in the literature.

We consider an array of Helmholtz resonators in a cylindrical duct of fixed geometric mean  $\delta = \sqrt{\delta_1 \delta_2} = 8.5$  mm of longitudinal and azimuthal inter-hole distances  $\delta_1$  and  $\delta_2$  (the model depends on  $\delta$ , not on  $\delta_1$  and  $\delta_2$  separately). The aperture of the Helmholtz resonator is a cylinder of diameter  $d_\delta = 1$  mm and height  $h_\delta = 1$  mm. The relative area of each resonator chamber is  $a_C = 0.9$  such that the area of cross section is  $a_C \delta^2 = 65.025$  mm<sup>2</sup>. We show results for different resonator depths  $L$ .

For all computations we consider the following physical parameters. The mean density of the air is  $\rho_0 = 1.2252$  kg m<sup>-3</sup>, the speed of sound is  $c = 340.45$  m s<sup>-1</sup> and the viscosity is  $\nu = 14.66 \times 10^{-6}$  m<sup>2</sup> s<sup>-1</sup>, see Tables A.3, A.4 and A.7 of Lahiri[27] for mean pressure  $p = 101.325$  kPa and temperature  $T = 288.15$  K.

### 4.1 Numerical computation of the effective Rayleigh conductivity

In this section, we describe how to compute numerically approximations of the solution  $(\mathbf{v}, p)$  of the characteristic problem (2.7) around one hole and from this an approximations to the effective Rayleigh conductivity. For this we consider the truncated domains  $\widehat{\Omega}(S)$  of radius  $S$  where we have to impose additional boundary conditions at the half spheres  $\Gamma_\pm(S)$ . It can be justified similarly to a previous study of a macroscopic problem with boundary layer effects[15] that acoustic velocity profile functions satisfies the decay condition  $\nabla \mathbf{v}^\top \mathbf{n} \rightarrow \mathbf{0}$  when  $|\mathbf{z}| \rightarrow \infty$ . Hence, we consider the *truncated characteristic problem* with homogeneous Neumann boundary conditions for  $\mathbf{v}_S$  on  $\Gamma_\pm(S)$ : Seek  $(\mathbf{v}_S, p_S) \in H^1(\widehat{\Omega}(S))^3 \times L^2(\widehat{\Omega}(S))$  solution of

$$\begin{aligned}
 -i\omega \mathbf{v}_S + \frac{1}{\rho_0} \nabla p_S - \nu_0 \Delta \mathbf{v}_S &= \mathbf{0}, & \text{in } \widehat{\Omega}(S), \\
 \text{div } \mathbf{v}_S &= 0, & \text{in } \widehat{\Omega}(S), \\
 \mathbf{v}_S &= \mathbf{0}, & \text{on } \partial \widehat{\Omega}(S) \cap \partial \widehat{\Omega}, \\
 \nabla \mathbf{v}_S^\top \mathbf{n} &= \mathbf{0}, & \text{on } \Gamma_\pm(S), \\
 p_S &= \pm \frac{1}{2}, & \text{on } \Gamma_\pm(S).
 \end{aligned} \tag{4.1}$$

The truncated characteristic problem is well-posed which can be similarly shown as the well-posedness of (2.7) (see proof of Proposition 2.1).

**Proposition 4.1.** *There exists a unique solution  $(\mathbf{v}_S, \mathbf{p}_S) \in \mathbf{H}^1(\widehat{\Omega}(S))^3 \times \mathbf{L}^2(\widehat{\Omega}(S))$  of (4.1).*

Following the formulation of the effective Rayleigh conductivity  $k_R$  defined by (2.9), we introduce the approximate effective Rayleigh conductivity  $k_R(S)$  as

$$k_R(S) := \frac{i\omega\rho_0}{2} \left( \int_{\widehat{\Gamma}_+(S)} \mathbf{v}_S \cdot \mathbf{n} - \int_{\widehat{\Gamma}_-(S)} \mathbf{v}_S \cdot \mathbf{n} \right).$$

We obtain an even more accurate approximation by computing  $k_R(S)$  for several values of  $S$  and an extrapolation for  $S \rightarrow \infty$  with a polynomial in  $1/S$ . In the examples in this section we computed for  $S = 40, 45, 50, 55, 60$ .

## 4.2 Study of the acoustic impedance and local resonance frequency

Following the works of Webster in the 1910s[55], the thesis of C. Lahiri[27] and the references within, the normalized specified acoustic impedance  $\zeta$  is defined by

$$\zeta := -\frac{\overline{p_0}}{c\rho_0\mathbf{v}_0 \cdot \mathbf{n}}. \quad (4.2)$$

Note that on our definition there is a complex conjugate and a change of sign as it was stated in our previous work[46].

For the impedance boundary condition given by the third line of (2.11) and by identification, the normalized specified acoustic impedance for array of Helmholtz resonators is given by

$$\zeta_{\text{AHM-3v}} := \frac{-\omega \text{Im}(k_R)}{c|k_R|^2} + i \left( \frac{\omega \text{Re}(k_R)}{c|k_R|^2} - \frac{1}{a_C} \cot \left( \frac{\omega L}{c} \right) \right), \quad (4.3)$$

the subscript AHM-3v stands for the proposed *three-scale asymptotic homogenization method with viscosity*.

We compare formula (4.3) with the most recent analytic formula taking into account viscosity (in a stagnant flow) in the acoustics literature, that is the formula of Guess[18]

$$\zeta_{\text{GUE}} = (1 + i) \frac{\sqrt{8\omega\nu}}{c\sigma} \left( 1 + \frac{h_\delta}{d_\delta} \right) + \frac{i\omega(h_\delta + \delta_{\text{COR}})}{c\sigma} + \frac{\omega^2 d_\delta^2}{8c^2\sigma} - \frac{i}{1-\varepsilon} \cot \left( \frac{\omega L}{c} \right), \quad (4.4)$$

extended by a correction  $1-\varepsilon$  for thickness of the side walls of the resonance chamber[26].

In view of (4.3) we choose  $\varepsilon = a_C$ . Here,  $\sigma := \pi d_\delta^2 / (4\delta^2)$  designates the porosity of the periodic array of apertures which takes value  $\sigma = 0.011$  in our study. Moreover,  $\delta_{\text{COR}}$  stands for the so-called end-point corrector for which different formulas exist in literature. We will use in our study the end-point corrector  $\delta_{\text{COR}} = 8d_\delta / (3\pi)$  of Morse[32] that takes the value  $\delta_{\text{COR}} = 0.849$  mm and of Ingard[24] based of a series expansion that takes the value  $\delta_{\text{COR}} = 0.709$  mm (when respecting the interaction with chamber walls through the parameter  $a_C$ ). Note that Ingard's approximate formula  $\delta_{\text{COR}} = 8d_\delta / (3\pi) (1 - 1.25\sqrt{\sigma/\pi}(1 + 1/\sqrt{a_C}))$  with two terms gives  $\delta_{\text{COR}} = 0.720$  mm and so almost the same value, and, hence, we use only Ingard's original formula. The end-point correction  $\delta_{\text{COR}} = 8d_\delta / (3\pi) (1 - 0.7\sqrt{\sigma})$  used by Guess[18] seems to neglect the interaction with the chamber walls at all and we do not take it into account in the study.



As for the formula of Guess the normalized specified acoustic impedance  $\zeta_{\text{AHM-3v}}$  of our approach is a combination of an impedance of the aperture and a reactance of the Helmholtz resonator, where normalized specified acoustic resistance and reactance denote the real and imaginary part of the acoustic impedance  $\zeta$ , respectively. Hence, the resistance  $\text{Re}(\zeta_{\text{AHM-3v}})$  is – as for Guess’ model – independent of the resonator chamber depth  $L$ . For Guess’ model it is even independent of the choice of the end-point correction. It admits a pole when  $\frac{\omega L}{c}$  is a multiple of  $\pi$ , *i. e.*, when  $L$  corresponds to a multiple of  $\frac{\lambda}{2}$ , when denoting by  $\lambda := \frac{2\pi c}{\omega}$  the characteristic one-dimensional wavelength in the Helmholtz resonator. For the resonator depth  $L = 100$  mm in our study the poles of the impedance are multiples of 1702 Hz. Moreover, the resistance  $\text{Re}(\zeta_{\text{CKR-v}})$  is a positive quantity since  $\text{Im}(k_R) < 0$  thanks to Proposition 2.2, which is also the case for Guess’ model.

In Figure 6 and in Figure 7 we plot the reactance  $\text{Im}(\zeta)$  for a resonator depth  $L = 100$  mm and the resistance  $\text{Re}(\zeta)$  (that is independent of  $L$ ) for our model in comparison with the formula of Guess with end corrections by Morse and Ingard as functions of the frequency. The reactance curve of our model is close to the one of Guess for both end-point corrections, and closest to the end-point correction of Ingard. However, the resistance curves differ from Guess’ formula. The difference in resistance is the higher the lower is the frequency, for 367 Hz it is 19.1% and for 1800 Hz only 1.27%. We observe that the resistance  $\text{Re}(\zeta_{\text{CKR-v}})$  tends for  $\omega \rightarrow 0$  to a positive constant, that is  $\text{Re}(\zeta_{\text{AHM-3v}}) = 0.1947$  in our study, where  $\zeta_{\text{GUE}}$  of Guess’ model tends to zero. Though, the low-frequency behaviour of Guess’ model seems to be unphysical, which is most likely based on the wrong assumption that the quantity  $\sqrt{\nu/\omega}$  is uniformly

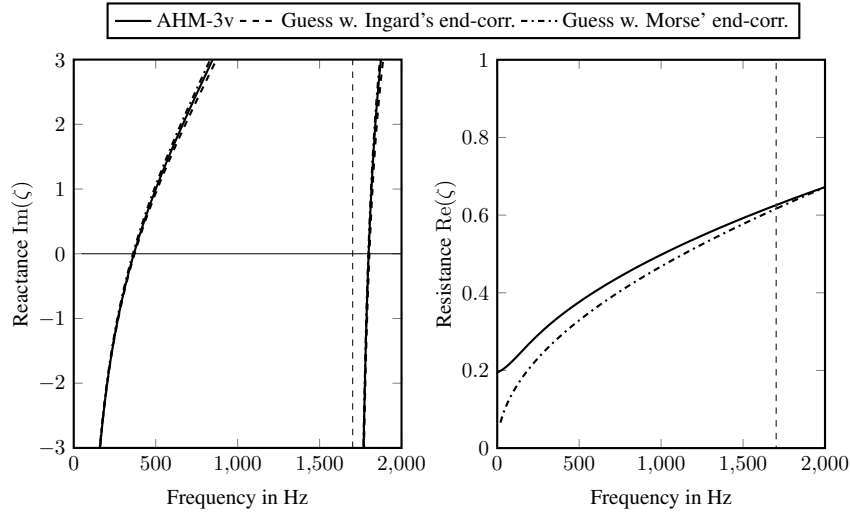


Figure 6: Reactance  $\text{Im}(\zeta)$  (*left*) and resistance  $\text{Re}(\zeta)$  (*right*) in dependence of frequency  $f = \frac{\omega}{2\pi}$  for  $d_\delta = h_\delta = 1$  mm,  $\delta = 8.5$  mm,  $L = 100$  mm and  $a_C = 0.9$ . Note that the resistance is independent of  $L$  for all models and for Guess’ model independent of the end-correction. The vertical line correspond to  $\lambda/2 = 1702$  Hz where the reactance  $\text{Im}(\zeta)$  admits a pole and the array of Helmholtz resonators acts as a sound-hard wall.

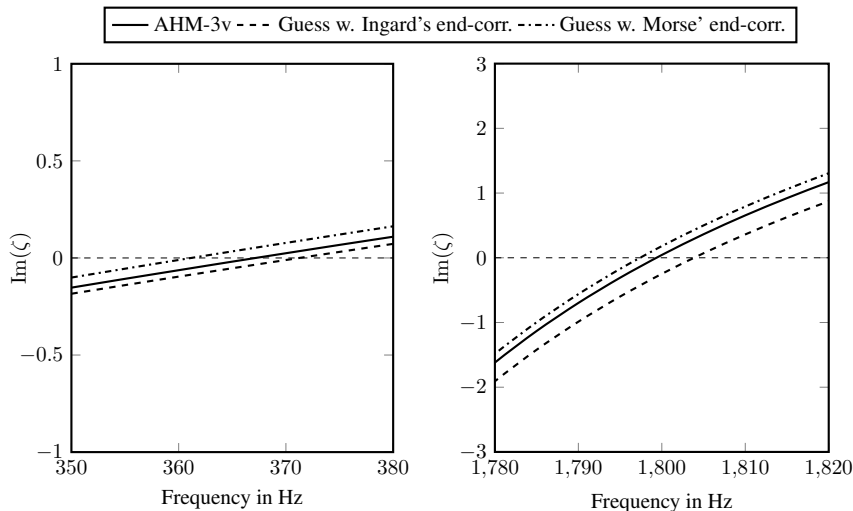


Figure 7: Reactance  $\text{Im}(\zeta)$  as as function of frequency in a neighborhood of the first (*left*) and second (*right*) characteristic frequency.

small in  $\omega$ .

In the view of the works of Panton and Miller[36] the resonance frequencies are the roots of  $\text{Im}(\zeta)$ . Guess' model predicts the first resonance frequency with 5 Hz lower using Morse' end-correction and 4 Hz higher using Ingard's end-correction than AHM-3v. The second resonance frequency predicted by Guess' model is 2 Hz lower using Morse' end-correction and 5 Hz higher using Ingard's end-correction than our model.

### 4.3 Dissipation by an array of Helmholtz resonators in a duct

Now, we simulate the transmission of a liner in an acoustic test duct (see[40] for fundamentals of duct acoustics) with circular cross-section with a radius  $R_d = 70$  mm (see Fig. 8). The geometrical setting is similar to previous studies[27, 46] on the duct DC006, where we replace the side chamber by an array of Helmholtz resonators. We call therefore the setting DC006\*. This array of Helmholtz resonators has a total length  $Z = 69$  mm and the other geometrical parameters were described in the beginning of this section. We model the array by the impedance boundary conditions in (2.12) and compare it to the boundary conditions according to Guess' impedance formula.

	resonance frequencies		dissipation maxima	
	first	second	first	second
AHM-3v	367 Hz	1799 Hz	359 Hz	1793 Hz
Guess w. Morse' end-corr.	362 Hz	1797 Hz	351 Hz	1791 Hz
Guess w. Ingard's end-corr.	371 Hz	1804 Hz	360 Hz	1797 Hz

Table 1: Resonance frequencies that corresponds to zeros of  $\text{Im}(\zeta)$  and dissipation maxima for liner DC006\* for a resonator chamber depth  $L = 100$  mm.

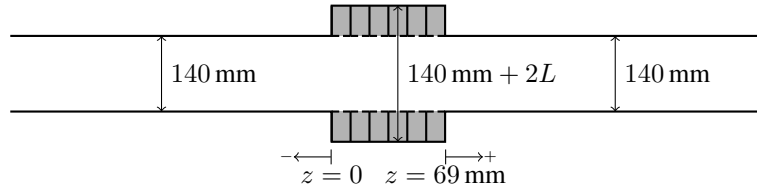


Figure 8: Considered domain for the duct acoustics. The grey region corresponds to the array of Helmholtz resonators.

We use the formulation for the acoustic pressure, see (2.12), with a source term corresponding to an incoming field  $p_{\text{inc}}(r, \theta, z) = \exp(i\omega z/c)$  from the left. The scattered field is computed numerically using the mode matching procedure as described in a previous work[52] with  $N = 5$  radial modes. We computed the eigenmodes numerically using the C++ Finite Elements Library CONCEPTS[17, 13].

We are interested in the energy dissipation of the liner that is defined as

$$D := 1 - T - R,$$

where  $T$  is the total transmitted energy and  $R$  is the total reflected energy. The energy dissipation is a global measure that depends on the damping properties of the array of Helmholtz resonators as well as on wave profile and macroscopic geometric settings.

We plot in Fig. 9 the energy dissipation for resonator chamber depths  $L = 50$  mm, 100 mm, 200 mm as functions of frequency for the proposed method AHM-3v. The observe the first maximum of energy dissipation at 240 Hz for  $L = 200$  mm, at 359 Hz for  $L = 100$  mm and at 530 Hz for  $L = 50$  mm, so at lower frequency for deeper resonator chambers (while keeping the cross-section). These frequencies are slightly below the first resonance frequencies, which are at 235 Hz for  $L = 200$  mm, at 367 Hz for  $L = 100$  mm

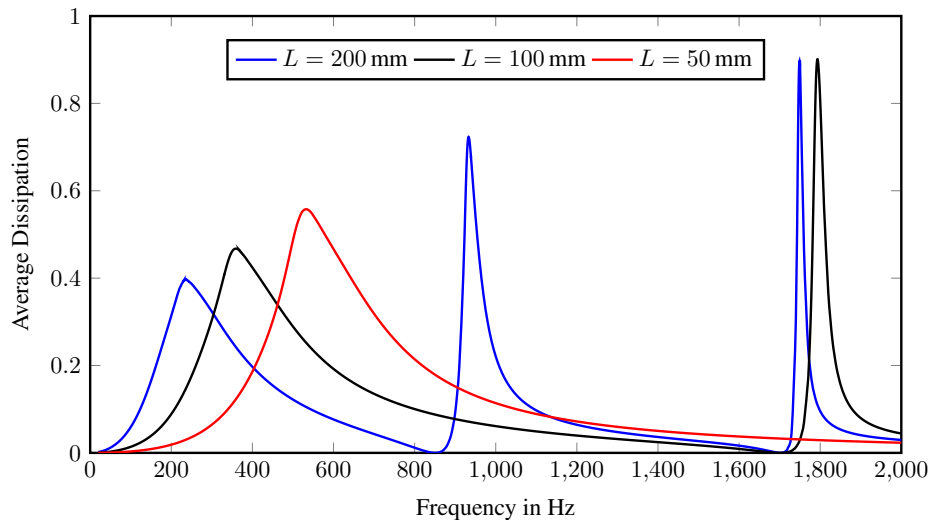


Figure 9: Numerically computed average dissipation for the liner DC006\* using the impedance model AHM-3v for different resonator depths  $L$ .

and at 533 Hz for  $L = 50$  mm. The amplitude at the first energy dissipation maximum is the higher the smaller the resonator chamber depth  $L$ . Independent of the latter the energy dissipation goes to 0 when decreasing the frequency to 0.

There is a first minimum of energy dissipation at 851 Hz for  $L = 200$  mm and at 1702 Hz for  $L = 100$  mm where the resonator chamber depth coincides with  $\lambda/2$ , where again  $\lambda$  is the wave-length. Here, the energy dissipation is 0 as the impedance boundary conditions becomes acoustic hard-wall conditions, *i. e.*, Dirichlet boundary conditions for the normal component of the velocity, and the incident field is passing the liner entirely transmitted. These frequencies correspond to poles of  $\text{Im}(\zeta_{\text{CKR-v}})$  and are equal with those predicted by the model of Guess' regardless of the choice of end-correction.

The second maxima of energy dissipation follows shortly the first minimum. It is observed at 930 Hz for  $L = 200$  mm and at 1793 Hz for  $L = 100$  mm, and, hence, again shortly below the second resonance frequencies which are at 933 Hz for  $L = 200$  mm and at 1799 Hz for  $L = 100$  mm. Another energy dissipation minimum is observed for  $L = 200$  mm at 1702 Hz followed by a maximum at 1750 Hz, which is again shortly below the third resonance frequency 1749 Hz.

We plot in Fig. 10 the energy dissipation curves for resonator chamber length  $L = 100$  mm in frequency windows around the first and second maximum, this for the proposed method AHM-3v together with those using the model of Guess with end-correctors of Morse and Ingard. The vertical lines correspond to the respective resonance frequencies (see Table 1), *i. e.*, to the roots of the reactance  $\text{Im}(\zeta)$  of the respective impedance. The observed energy dissipation maxima are very close for the

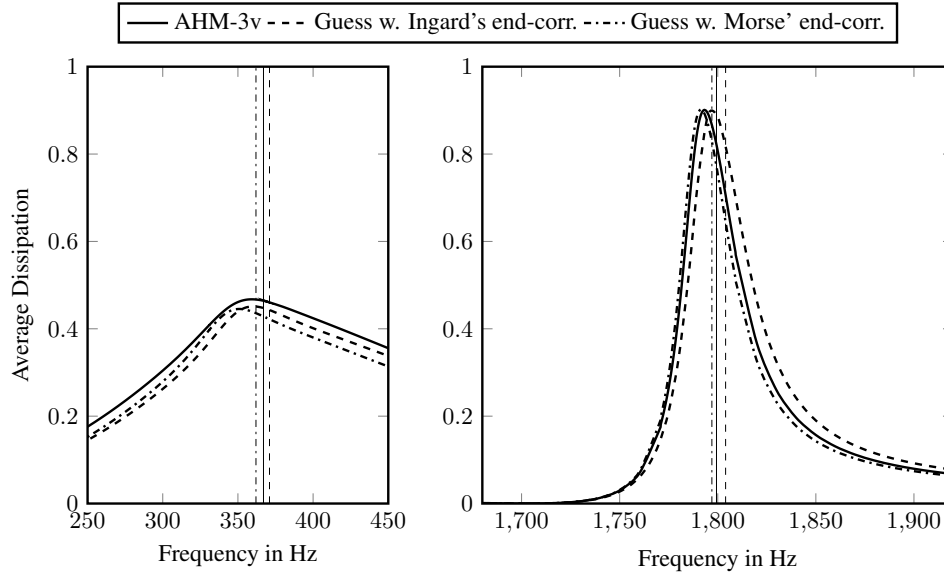


Figure 10: Numerically computed average dissipation for the liner configuration DC006\* for the model AHM-3v and the models from Rienstra and Guess close to the first (*left*) and second (*right*) resonance frequencies (see Table 1) that are shown by vertical lines. The diameter of the hole is  $d_\delta = 1$  mm and the resonator depth is  $L = 100$  mm.

different models (see Table 1), for Guess' model with Ingard's correction it is only about 2, Hz lower for the first and about 4 Hz higher for the second maximum than the proposed model AHM-3v. The predicted energy dissipation at the first maximum is around 3 % lower for Guess' model with Ingards end corrector and around 5 % lower with Morse' end corrector than for the proposed model AHM-3v. This seems to be the consequence of the difference in resistance of the formulas. Around the second dissipation maxima the dissipation curves of the different models are very close confirming that prediction of the first maximum is most severe.

## Conclusion

We presented impedance boundary conditions that can be used to predict the damping properties as well as the resonance frequencies of periodic arrays of elongated Helmholtz resonators for low acoustic amplitudes in a stagnant gas. Considering a period  $\delta$  that is small in comparison to the wave-length and even smaller diameter of the orifices, scaled as  $\delta^2$ , and small viscosity that is scaled like  $\delta^4$  we obtain a non-trivial limit for  $\delta \rightarrow 0$ , in difference to an homogenization with only two geometric scales, cf. [8, 51]. In this way the dominating effects are considered on each geometric scale, that are viscous effects and incompressible acoustic velocity around each hole, only incompressibility in an intermediate zone above and below the perforated plate, one-dimension wave-propagation inside the resonance chamber and pure acoustics wave-propagation away from the perforated plate. The separation of the scales give a choice of the viscous region, in difference to the approach by Lidoine *et al.* [30].

It turns out that the impedance boundary conditions depend mainly on effective Rayleigh conductivity of the multiperforated plate[46] and the reactance of the resonance chambers. The effective Rayleigh conductivity can be approximately computed by discretizing of a canonical problem in two half spaces separated by an wall of finite thickness except for a single hole, where the infinite domain has to be truncated.

The derivation of the impedance boundary conditions is based on the two-scale convergence[35, 1], which is to our knowledge the first time applied to a periodic transmission problem. The application of the two-scale convergence makes the proof of convergence less technical in comparison to the method of matched asymptotic expansions or the method of multiscale analysis, where viscous boundary layers and the singular behaviour close to all edges of the geometry have to be considered. However, the justification is based on a stability assumption for the  $\delta$ -dependent problem that shall be proved in a forthcoming article.

In numerical simulations we have compared the derived impedance and computed dissipation with an established model [18] of the acoustics community. The approach allows to integrate further effects as nonlinear convection for higher sound amplitudes or a gracing or bias flow.

## 5 References

- [1] G. Allaire, Homogenization and two-scale convergence, *SIAM J. Appl. Math.* **23** (1992) 1482–1518.
- [2] H. Ammari and H. Zhang, A mathematical theory of super-resolution by using a system of sub-wavelength Helmholtz resonators, *Communications in Mathematical Physics* **337** (2015) 379–428.

- [3] V. Andreev and N. Kopteva, Pointwise approximation of corner singularities for a singularly perturbed reaction-diffusion equation in an L-shaped domain, *Math. Comp.* **77** (2008) 2125–2139.
- [4] Y. Aurégan, R. Starobinski and V. Pagneux, Influence of grazing flow and dissipation effects on the acoustic boundary conditions at a lined wall, *J. Acoust. Soc. Am.* **109** (2001) 59–64.
- [5] A. Bendali, M. Fares, S. Laurens and S. Tordeux, Numerical study of acoustic multiperforated plates, *ESAIM: Proc.* **37** (2012) 166–177.
- [6] A. Bendali, M. Fares, E. Piot and S. Tordeux, Mathematical justification of the rayleigh conductivity model for perforated plates in acoustics, *SIAM J. Numer. Anal.* **73** (2013) 438–459.
- [7] M. Berggren, A. Bernland and D. Noreland, Acoustic boundary layers as boundary conditions, *J. Comput. Phys.* **371** (2018) 633 – 650.
- [8] A.-S. Bonnet-BenDhia, D. Drissi and N. Gmati, Mathematical analysis of the acoustic diffraction by a muffler containing perforated ducts, *Math. Models Meth. Appl. Sci.* **15** (2005) 1059–1090.
- [9] D. Braess, *Finite Elements: Theory, Fast Solvers, and Applications in Solid Mechanics* (Cambridge University Press, 2007), 3th edition.
- [10] F. Brezzi, On the existence, uniqueness and approximation of saddle-point problems arising from lagrangian multipliers, *Rev. fr. autom. inform. rech. opér. , Anal. numér.* **8** (1974) 129–151.
- [11] F. Brezzi and M. Fortin, *Mixed and hybrid finite element methods* (Springer, Berlin & Heidelberg, Germany, 1991).
- [12] X. Claeys and B. Delourme, High order asymptotics for wave propagation across thin periodic interfaces, *Asymptot. Anal.* **83** (2013) 35–82.
- [13] Concepts Development Team, *Webpage of Numerical C++ Library Concepts 2* (<http://www.concepts.math.ethz.ch>, 2020).
- [14] B. Delourme, H. Haddar and P. Joly, Approximate models for wave propagation across thin periodic interfaces, *J. Math. Pures Appl. (9)* **98** (2012) 28–71.
- [15] B. Delourme, K. Schmidt and A. Semin, On the homogenization of thin perforated walls of finite length, *Asymptotic Analysis* **97** (2016) 211–264.
- [16] L. C. Evans, *Weak convergence methods for nonlinear partial differential equations*, 74 (American Mathematical Soc., 1990).
- [17] P. Frauenfelder and C. Lage, Concepts – An Object-Oriented Software Package for Partial Differential Equations, *ESAIM: Math. Model. Numer. Anal.* **36** (2002) 937–951.
- [18] A. Guess, Calculation of perforated plate liner parameters from specified acoustic resistance and reactance, *J. Sound Vib.* **40** (1975) 119–137.
- [19] H. Helmholtz, *Die Lehre von den Tonmpfindungen als physiologische Grundlage für die Theorie der Musik* (Vieweg und Sohn, Braunschweig, 1863).

- [20] E. W. Hobson, *The theory of spherical and ellipsoidal harmonics* (Chelsea Pub. Co., 1955).
- [21] M. S. Howe, The influence of grazing flow on the acoustic impedance of a cylindrical wall cavity, *J. Sound Vib.* **67** (1979) 533–544.
- [22] M. S. Howe and M. S. Howe, *Acoustics of fluid-structure interactions* (Cambridge Monographs on Mechanics. Cambridge university press, Boston University, 1998).
- [23] D. Iftimie and F. Sueur, Viscous boundary layers for the Navier–Stokes equations with the Navier slip conditions, *Arch. Ration. Mech. Anal.* **1** (2010) 39.
- [24] U. Ingard, On the theory and design of acoustic resonators, *J. Acoust. Soc. Am.* **25** (1953) 1037–1061.
- [25] U. Ingard and H. Ising, Acoustic nonlinearity of an orifice, *J. Acoust. Soc. Am.* **48** (1967) 6–16.
- [26] J. Kooi and S. Sarin, An experimental study of the acoustic impedance of helmholtz resonator arrays under a turbulent boundary layer, in *7th Aeroacoustics Conference* (1981), p. 1998.
- [27] C. Lahiri, Acoustic performance of bias flow liners in gas turbine combustors, Ph.D. thesis, Technische Universität Berlin, Berlin, Germany, 2014.
- [28] L. D. Landau and E. M. Lifshitz, *Fluid Mechanics*, Course of theoretical physics / by L. D. Landau and E. M. Lifshitz, Vol. 6 (Pergamon press, New York, 1959), 1st edition.
- [29] R. Leis, *Initial Boundary Value Problems in Mathematical Physics* (B. G. Teubner GmbH, 1986).
- [30] S. Lidoine, I. Terrasse, T. Abboud and A. Bennani, Numerical prediction of SDOF-Perforated Plate Acoustic Treatment Impedance. Part 1: Linear domain, *13 th AIAA/CEAS Aeroacoustics Conference* .
- [31] V. Lukěš and E. Rohan, Modelling of acoustic transmission through perforated layer, *Appl. Comp. Mech.* **1** (2007) 137–142.
- [32] P. M. Morse, *Vibration and sound*, volume 2 (McGraw-Hill New York, 1948).
- [33] C.-D. Munz, M. Dumbser and S. Roller, Linearized acoustic perturbation equations for low mach number flow with variable density and temperature, *J. Comput. Phys.* **224** (2007) 352–364.
- [34] S. A. Nazarov, Neumann problem in angular domains with periodic boundaries and parabolic perturbations of the boundaries, *Trans. Moscow Math. Soc.* **69** (2008) 153–208.
- [35] G. Nguetseng, A general convergence result for a functional related to the theory of homogenization, *SIAM J. Appl. Math.* **20** (1989) 608–623.
- [36] R. L. Panton and J. M. Miller, Resonant frequencies of cylindrical Helmholtz resonators, *J. Acoust. Soc. Am.* **57** (1975) 1533–1535.

- [37] M. H. Protter, Unique continuation for elliptic equations, *Trans. Amer. Math. Soc.* **95** (1960) 81–91.
- [38] L. Rayleigh, On the theory of resonances, *Phil. Trans. Roy. Soc. London* **161** (1870) 77–118.
- [39] L. Rayleigh, *The theory of sound (volume 2)* (Dover, New York, 1945).
- [40] S. W. Rienstra, Fundamentals of duct acoustics, Von Karman Institute Lecture Notes, Nov 2015.
- [41] S. W. Rienstra and M. Darau, Boundary-layer thickness effects of the hydrodynamic instability along an impedance wall, *J. Fluid. Dynam.* **671** (2011) 559–573.
- [42] S. W. Rienstra and A. Hirschberg, *An Introduction to Acoustics* (Eindhoven University of Technology, Eindhoven, 2018).
- [43] S. W. Rienstra and D. K. Singh, Nonlinear Asymptotic impedance Model for a Helmholtz Resonator of Finite Depth, *AIAA Journal* **56** (2018) 1792–1802.
- [44] J. Sanchez-Hubert and E. Sanchez-Palencia, Acoustic fluid flow through holes and permeability of perforated walls, *J. Math. Anal. Appl.* **87** (1982) 427 – 453.
- [45] S. Sauter and C. Schwab, *Boundary element methods* (Springer, Berlin & Heidelberg, Germany, 2011).
- [46] K. Schmidt, A. Semin, A. Thöns-Zueva and F. Bake, On impedance conditions for circular multiperforated acoustic liners, *J. Math. Ind.* **8** (2018) 15.
- [47] K. Schmidt, A. Thöns-Zueva and P. Joly, Asymptotic analysis for acoustics in viscous gases close to rigid walls, *Math. Models Meth. Appl. Sci.* **24** (2014) 1823–1855.
- [48] A. Schulz, Die akustischen Randbedingungen perforierter Wandauskleidungen in Strömungskanälen, Ph.D. thesis, Technische Universität Berlin, Berlin, Germany, 2018.
- [49] B. Schweizer, The low-frequency spectrum of small Helmholtz resonators, *Proc. R. Soc. Lond. A* **471** (2015) 20140339.
- [50] A. Semin, B. Delourme and K. Schmidt, On the homogenization of the Helmholtz problem with thin perforated walls of finite length, *ESAIM: Math. Model. Numer. Anal.* **52** (2018) 29–67.
- [51] A. Semin and K. Schmidt, On the homogenization of the acoustic wave propagation in perforated ducts of finite length for an inviscid and a viscous model, *Proc. R. Soc. Lond. A* **474**.
- [52] A. Semin, A. Thöns-Zueva and K. Schmidt, Simulation of reflection and transmission properties of multiperforated acoustic liners, in *Progress in Industrial Mathematics at ECMI 2016*, ed. P. et al. Quintela (Springer International Publishing, Cham, Switzerland, 2017), volume 26 of *Mathematics in Industry*, pp. 69–76.
- [53] D. K. Singh and S. W. Rienstra, Nonlinear asymptotic impedance model for a helmholtz resonator liner, *J. Sound Vib.* **333** (2014) 3536–3549.



- [54] C. K. W. Tam and K. A. Kurbatskii, Microfluid dynamics and acoustics of resonant liners, *AIAA Journal* **38** (2000) 1331–1339.
- [55] A. G. Webster, Acoustical impedance and the theory of horns and of the phonograph, *Proc. Natl. Acad. Sci. U. S. A.* **5** (1919) 275.